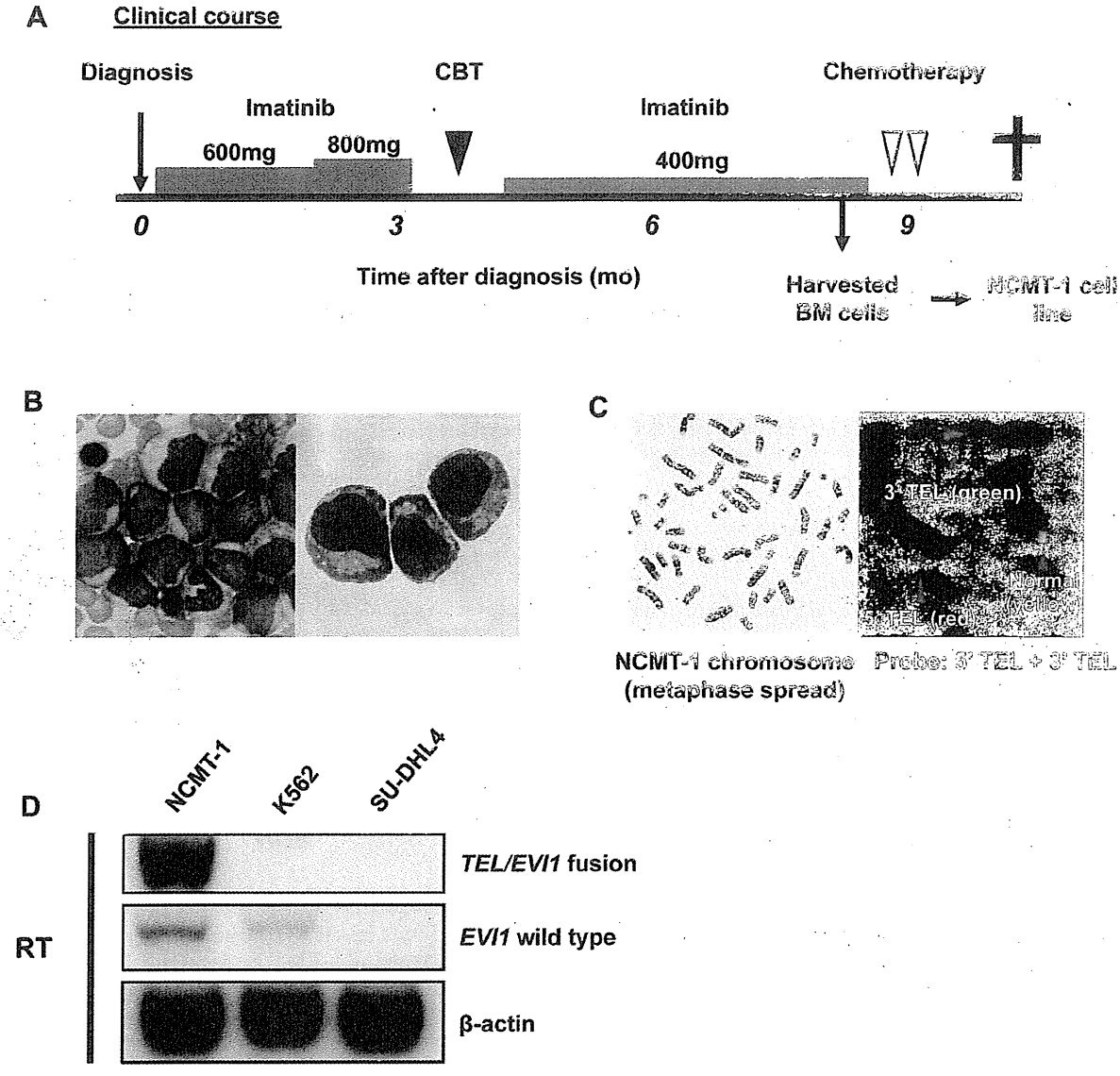

Figure 1. Clinical course of a patient with CML who was resistant to imatinib and molecular characterization of the NCMT-1 cell line. (**A**) A 36-year-old female was admitted to the affiliated hospital of Nagoya University in September 2005 and diagnosed with CML in blast crisis. The flow cytometric analysis revealed CD13, CD33, CD34, and HLA-DR positivity on her tumor cells. A 600-mg dose of imatinib was administered as the first line of therapy. Failure to obtain a full hematologic response resulted in a dose escalation to 800 mg during this first course of treatment. A complete hematological response was finally achieved, however, no cytogenetic response and no major molecular response were observed. Subsequently, 3 months after diagnosis, the patient received a cord blood stem cell transplant (CBT) (black triangle), but the bone marrow at the recovery phase of the transplant still included tumor cells. Imatinib was administered again after CBT, but her condition continued to deteriorate even during treatment. Finally, she received palliative chemotherapy (white triangle) and died of her disease in June 2006. (**B**) Bone marrow aspirate smear from a diagnostic sample from the patient (left panel) or cytospin specimens of NCMT-1 cells (right panel) stained with May-Grünwald-Giemsa staining and examined microscopically. Blast cells with Azur granules are clearly seen in the specimens. (**C**) Chromosomal analysis of the NCMT-1 cell line revealed a complicated karyotype, including 3q26 abnormalities and t(9;22)(q34;q11.2) in G-banding analysis (left panel), and a split signal of the 5′ and 3′ *TEL* gene probes in fluorescence in situ hybridization analysis (right panel), indicating maintenance of the t(3;12)(q26;p13) translocations in the NCMT-1 cells. (**D**) Reverse transcriptase (RT) PCR analysis of NCMT-1, K562, and SU-DHL4 cells. Complementary DNA from each cell line was prepared and then subjected to PCR using primers to *TEL* and *EVI1* to detect the fusion gene or *EVI1* alone to detect the wild-type product. A single band indicating the *TEL/EVI1* fusion was detected in NCMT-1, but not K562 or SU-DHL4 cells. Using EVI1-U and EVI-L primers, the *EVI1* wild-type band was also detected in NCMT-1 and K562 cells. A PCR reaction using primers for β-actin was also performed as an inter-sample and loading control.

the bone marrow niche, activation of other oncogenes (e.g., LYN) [13,14], or tumor dormancy [15,16]. Treatment in each case becomes far more difficult, and so uncovering means of overcoming resistance is vital.

During disease development and in chronic phase, the initiating lesion BCR-ABL is thought to cause genetic instability, resulting in additional genetic abnormalities in genes associated with proliferation, differentiation, and

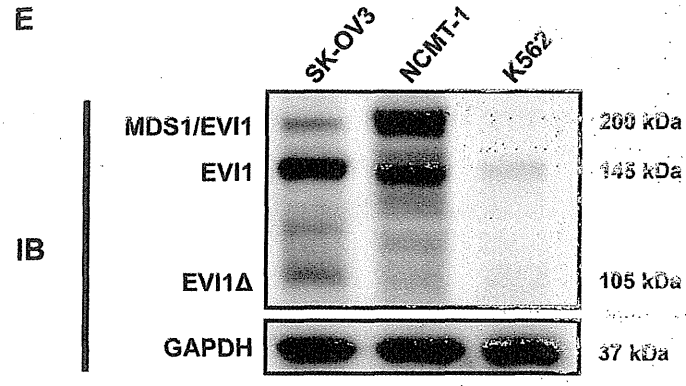

Figure 1. (*Continued*) (**E**) Immunoblotting (IB) analysis of NCMT-1 and K562 cells. Whole cell lysates were prepared from each cell line and assessed by immunoblotting for MDS1/EVI1 or glyceraldehyde phosphate dehydrogenase (GAPDH). Expression of the fusion protein (200 kDa) was strongly detected in NCMT-1 but not K562 cells. The wild-type EVI1 band (145 kDa) was also detected although expression was lower than the fusion protein. SK-OV3 was used as a positive control of EVI1 protein. GAPDH was used as a loading control on the same membrane.

apoptosis [1]. Typically, chromosomal abnormalities including trisomy 8 and translocations of other oncogenes are acquired [17]. These additional abnormalities are thought to cause resistance to TKI and impair treatment.

EVI1 (ectopic viral integration site 1) is a transcription factor with two zinc finger motifs, and its acquisition is known to be a poor prognostic factor for acute myeloid leukemia [18]. *EVI1* is located on 3q26, and aberrant expression is mainly mediated by the t(3;3)(q21;q26), inv(3)(q21q26), t(3;12)(q26;p13), and t(3;21)(q26;q22) genomic aberrations [19–21]. The t(3;12)(q26;p13) resulting in the *TEL/MDS1/EVI1* fusion is reported in CML, acute myeloid leukemia, and myelodysplastic syndrome [22]. EVI1 itself is indispensable for proliferation of hematopoietic stem cells [23] and possesses various oncogenic functions, including suppression of transforming growth factor–β [24], negative regulation of the c-Jun N-terminal kinase pathway [25], and stimulation of cell growth by *AP-1* [26]. However, its impact on apoptotic regulation has not been well studied.

Here we report on the establishment of a novel CML cell line derived from a patient who developed CML in blast crisis and was refractory to various treatments, including TKI and stem cell transplantation. The tumor at diagnosis indicated t(3;12)(q26;p13) as an additional chromosomal abnormality, and this was retained in the established cell line. The cell line also retained resistance to TKI, providing us with a valuable tool for understanding the mechanism of TKI resistance and allowing us to investigate the contribution of the t(3;12)(q26;p13) in this. Using *EVI1*-specific small interfering RNA (siRNA), we were able to reduce expression of the fusion protein and show that resistance was due, at least in part, to the inhibition of BAD by AKT downstream of EVI1 signaling. We were also able to show that TKI resistance could be overcome by addition of the BH3-mimetic, ABT-737, or an AKT inhibitor, indicating two separate approaches that might offer better treatment strategies for EVI1-overexpressing leukemias resistant to TKI.

Material and methods

Chemicals, reagents, and cell lines

Imatinib was supplied by Novartis (Basel, Switzerland). Dasatinib was supplied by Bristol-Myers Squibb (New York, NY, USA). AKT inhibitor VIII was purchased from Merck (Nottingham, UK). K562 were obtained from the ATCC (Manassas, VA, USA). All cultures were monitored routinely and found to be free of mycoplasma.

Clinical history and establishment of the NCMT-1 cell line

A 36-year-old female was admitted to Ogaki Municipal Hospital and diagnosed with CML in blast crisis. She was administered imatinib (600 mg) immediately following diagnosis and then a higher dose (800 mg) during treatment to achieve a hematological response, but a full cytogenetic response was not observed. A <1-log reduction of tumor was observed by quantitative polymerase chain reaction (PCR) [27]. Following the failure of imatinib, the patient received a cord blood stem cell transplant, but this did not arrest the disease. Subsequently, imatinib was re-administered, but it again failed to fully control the disease and the patient died 9 months after diagnosis. Bone marrow cells obtained at the refractory phase after transplantation were subsequently used to establish a cell line. Mononuclear cells were purified with Ficoll-Conray solution and cultured in Iscove's modified Dulbecco's medium (Sigma Aldrich, St Louis, MO, USA) supplemented with 20% fetal calf serum. The medium was changed every 1 to 2 weeks. After observing prolonged growth, the cell line (termed *NCMT-1*) was considered established and the fetal calf serum concentration reduced to 10%.

Cytogenetic analysis

Chromosomal G-banding was performed by the Mitsubishi Chemical Medience Corporation (Tokyo, Japan). TEL gene translocation was analyzed by fluorescence in situ hybridization by SRL, Inc. (Tokyo, Japan).

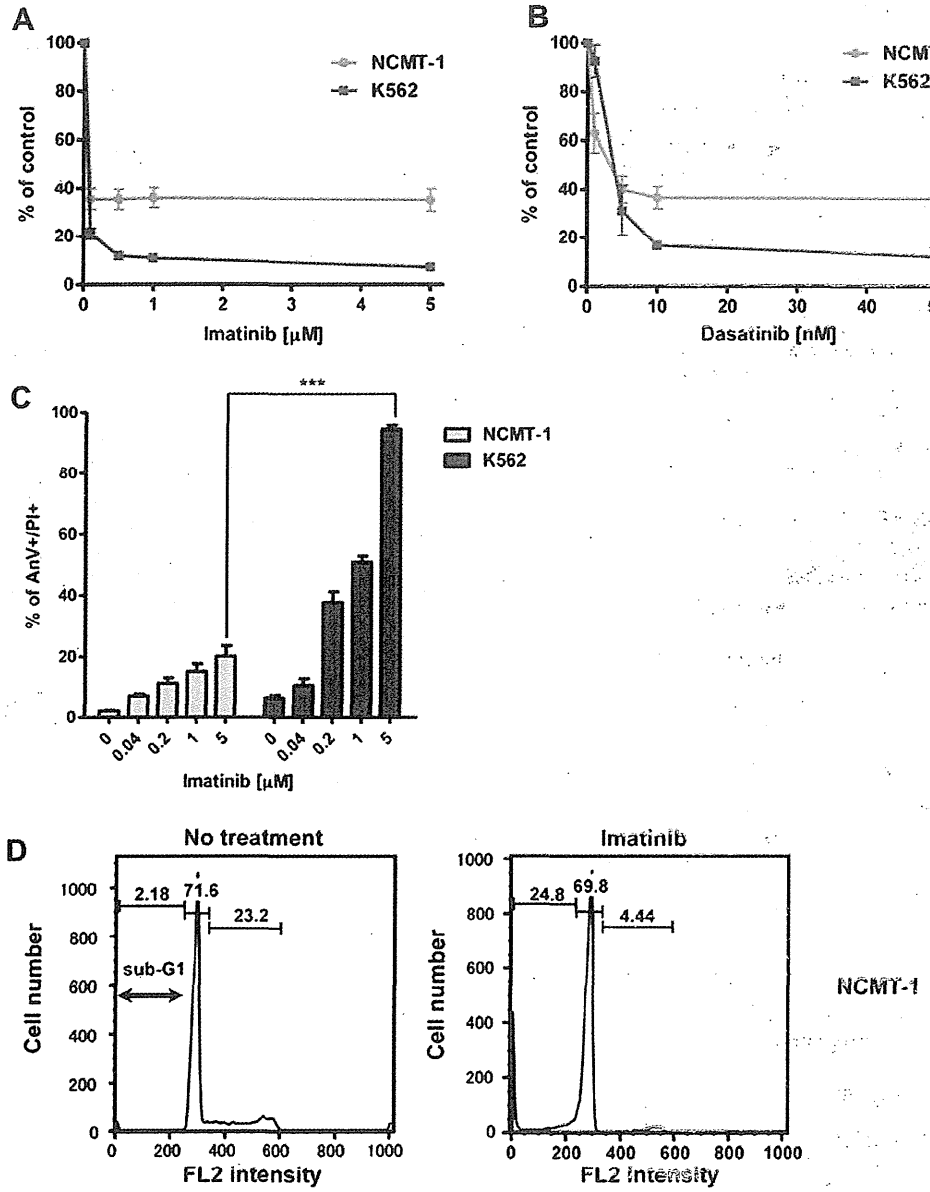

Figure 2. NCMT-1 cells have partial resistance to TKI. (**A**, **B**) To evaluate cell proliferation in the presence of various concentrations of TKI, the MTT assay was performed on K562 or NCMT-1 cells after 72 h of incubation in the presence of imatinib (0.1, 0.5, 1, and 5 μM) (**A**), or dasatinib (1, 5, 10, and 50 nM) (**B**). Inhibition of cell proliferation in NCMT-1 cells (gray circles) is clearly less than that observed with K562 cells (black squares) with both TKIs. Each point represents the mean value taken from three independent experiments, with error bars indicating the standard error of the mean (SEM). (**C**) Death assay in NCMT-1 and K562 cells after imatinib treatment. After 48-h incubation in the presence of various concentrations of imatinib (0, 0.04, 0.2, 1, and 5 μM), Annexin V (AnV)-FITC/PI cell death assays were performed. The amount of cell death induced in NCMT-1 cells was clearly less than induced in K562 cells ($p < 0.0001$ at 5 μM). Each point represents the mean value taken from three independent experiments, with error bars indicating SEM. (**D**, **E**) Cell cycle analysis after imatinib treatment. NCMT-1 (**D**) and K562. (**E**) cells were treated with 0.5 μM imatinib for 72 h, then lysed in hypotonic PI solution and assessed by flow cytometry. In NCMT-1 cells, the transition from the G_1 to the S and G_2/M phase was clearly inhibited in the presence of imatinib, indicative of cell cycle arrest (**D**).

RNA preparation, reverse transcriptase PCR, and DNA sequence analysis

Total RNA was extracted from cells using PureLink RNA Mini Kit (Invitrogen, Carlsbad, CA, USA) according to manufacturer's protocol. Complementary DNA was prepared with SuperScript III reverse transcriptase and random primers (Invitrogen). To detect the *TEL/EVI1* fusion, the *EVI1* wild-type gene transcript and β-actin messenger RNA, the primers listed in Supplementary Table E1 (online only, available at www.exphem.org) were used. Reverse transcriptase PCR with GoTaq hot start polymerase (Promega, Southampton, UK) was performed as described previously [28]. Images obtained with the GelDocXR

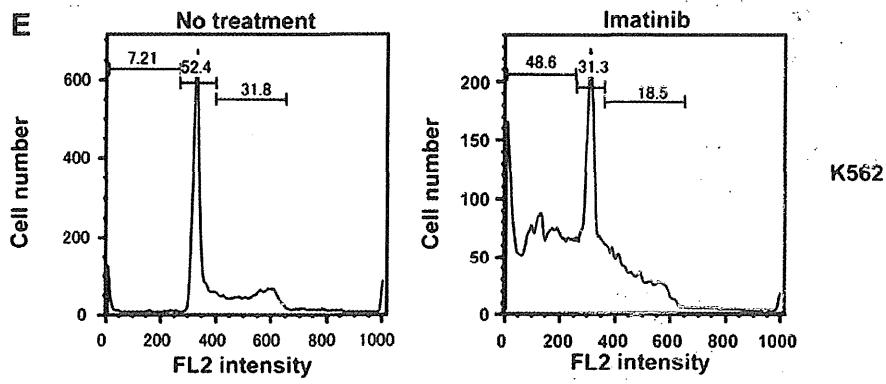

Figure 2. (*Continued*) In K562 (E) cells, the sub-G_1 population was far more evident compared to NCMT-1 cells.

imaging system (Bio-Rad, Hempstead, UK) were analyzed with Adobe Photoshop CS4 (Adobe Systems, San Jose, CA, USA). Sequencing was performed using the BigDye Terminator Cycle Sequencing Kit (Applied Biosystems, Foster City, CA, USA) and the product directly sequenced using an ABI 310 automated DNA sequencer (Applied Biosystems).

MTT assay

To evaluate cell proliferation, we performed MTT assays. Cells (2.5×10^4 for NCMT-1 and 1.0×10^4 for K562) were placed in 96-well plates and cultured for 72 h at 37°C in a 5% CO_2 incubator. Ten microliters TetraColor ONE (Seikagaku Biobusiness Corporation, Tokyo, Japan) was then added into each well and the fluorescence evaluated at 450 nM.

Cell death and cell cycle assessment

To evaluate cell death, the propidium iodide (PI) and Annexin V–fluorescein isothiocyanate (FITC) assay was performed as detailed previously [29]. Cells were placed in 96-well plates, incubated with the required drugs for 48 h, stained with 5 μg/mL PI and 1.6 μg/mL Annexin V-FITC for 15 min at room temperature in the dark, and cell death evaluated by flow cytometry (FACScan or FACSCalibur; BD, Franklin Lakes, NJ, USA). For cell cycle assessment, cells were assessed using the hypotonic PI assay detailed previously [30,31]. Cells were incubated for 72 h with imatinib, washed, and resuspended in phosphate-buffered saline containing 0.2% Triton X-100 and 50 μg/mL PI before analysis by flow cytometry as described.

Immunoblotting

Cells were treated as detailed and then lysed as described previously [32]. When required, 50 mM NaF and 1.68 mM Na_3VO_4 were added to prevent post-lysis changes in phosphorylation. After centrifugation (13,000 rpm for 10 min), sample buffer containing 5% 2-mercaptoethanol was added. After boiling for 5 min, samples were separated by sodium dodecyl sulfate polyacrylamide gel electrophoresis, transferred to polyvinyldene difluoride membranes and blocked with 5% skimmed milk in TBS-Tween buffer (50 mM Tris-HCl [pH 7.4], 150 mM NaCl and 0.05% Tween 20). Immunoblotting was carried out using primary antibodies (Supplementary Table E2; online only, available at www.exphem.org) appropriately diluted in TBS-Tween buffer with 5% bovine serum albumin and 0.05% sodium azide; horseradish peroxidase–conjugated secondary monoclonal antibodies (GE Healthcare, Chalfont St Giles, UK) were used as described and detected with Amersham ECL-plus (GE), Super-Signal West Pico (Thermo Scientific, Rockford, IL, USA) or Immobilon Western Substrate (Millipore, Billerica, MA, USA). Images obtained with the BioSpectrum AC system were analyzed with VisionWorksLS software (UVP, LLC, Cambridge, UK).

EVI1 knockdown

Transfection of siRNA (300 nM) was performed by Nucleofection using Amaxa Nucleofector Kit V (Lonza, Basel, Switzerland) according to manufacturer's protocol. siRNAs for *EVI1* were from Invitrogen (Stealth Select RNAi; Invitrogen) and control siRNA (Silencer Negative Control #1 siRNA) were from Applied Biosystems. Knock-down was confirmed by immunoblotting 48 h after transfection.

Statistical analysis

Statistical significance in the MTT and cell death assays was evaluated by unpaired *t* test using GraphPad PRISMv5 (GraphPad Software Inc. La Jolla, CA, USA). To calculate synergy, data was analyzed with CalcuSyn software (BIOSOFT, Cambridge, UK).

Results

Establishment of a CML cell line expressing the TEL/EVI1 fusion

During our routine clinical practice, we encountered a CML patient who was refractory to imatinib. The detailed clinical course of this patient and pathological specimens at her diagnosis are shown in Figure 1A, B. Given the unusual clinical course, we generated a cell line from the bone marrow cells obtained at the refractory phase ~8 months after diagnosis. A cell line, NCMT-1, developed (Fig. 1B, right panel). Chromosomal analysis revealed 46, XX, -1, der(1)?dup(1)(p13p22)inv(1)(p22q21)del(1)(q21q23), −2, add(3)(q26), add(6)(p23), t(9;22)(q34;q11.2), add(12)(p11.2), −20, +der(?)t(?;1)(?;q21), +2mar [20/20], indicating the continuing presence of the *EVI1* gene abnormality and *BCR-ABL* fusion in the clonal cell line (Fig. 1C, left panel).

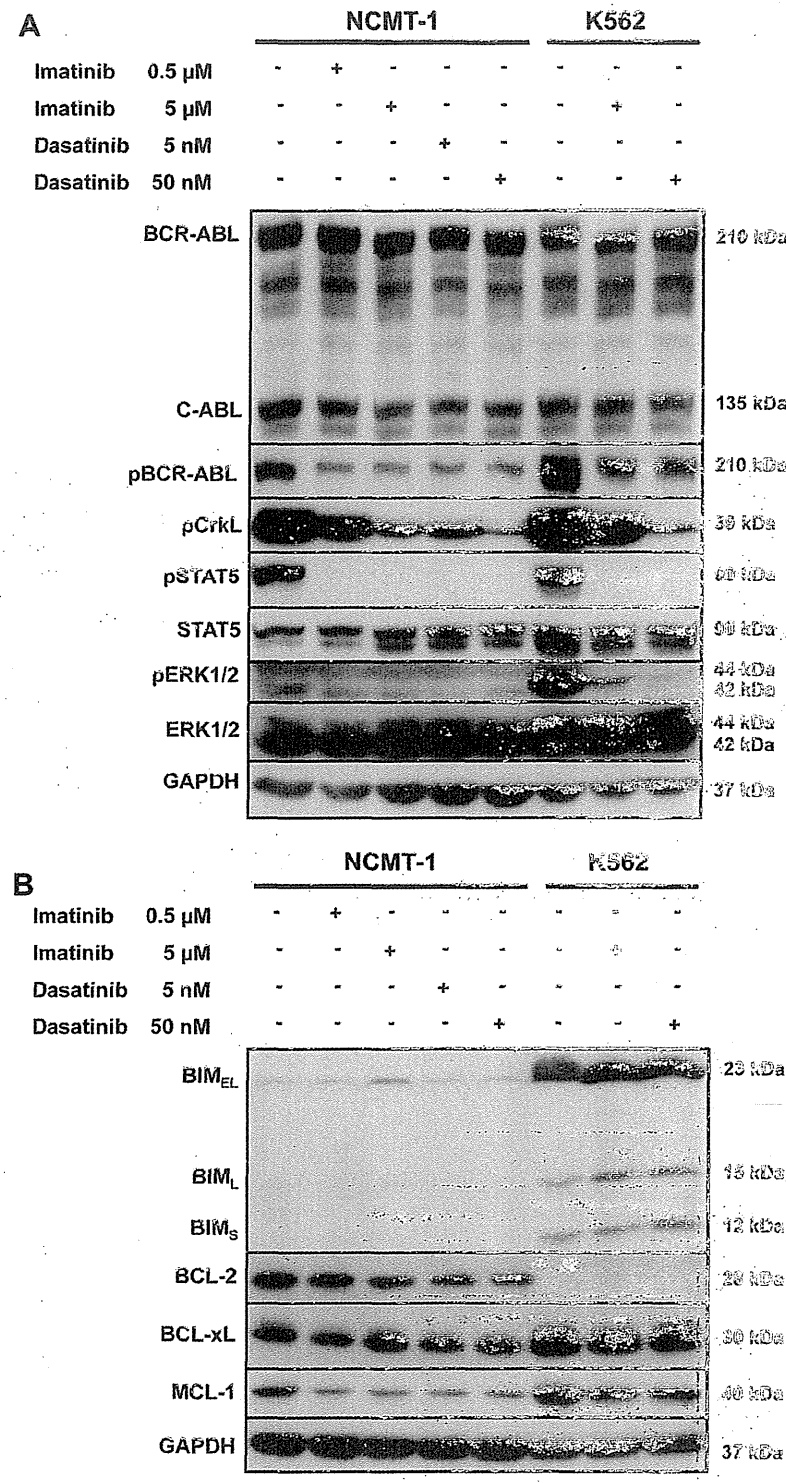

Figure 3. Immunoblotting analysis of NCMT-1 and K562 cells in the presence or absence of TKI. Whole cell lysates from each sample were obtained after 6-h incubation with TKI at the indicated dose, before analysis by immunoblotting. In both NCMT-1 cells, resistant to TKI, and K562 cells, sensitive to TKI, a similar signaling pathway downstream of BCR-ABL is in evidence, indicated by the dephosphorylation of BCR-ABL, CrkL, and signal transducers and activators of transcription (STAT) 5 after TKI treatment. (**A**) Analysis of signaling proteins: BCR-ABL, c-ABL, CrkL, STAT5, and glyceraldehyde phosphate dehydrogenase (GAPDH) as a loading control. (**B**) Analysis of apoptosis proteins: BIM, BCL-2, BCL-xL, MCL-1, and GAPDH as a loading control. BIM is less well expressed in NCMT-1 cells compared to K562 cells, and BCL-2 is expressed at high levels in NCMT-1 cells compared to K562 cells. All of the blotting was performed on membranes obtained from the same whole cell lysates.

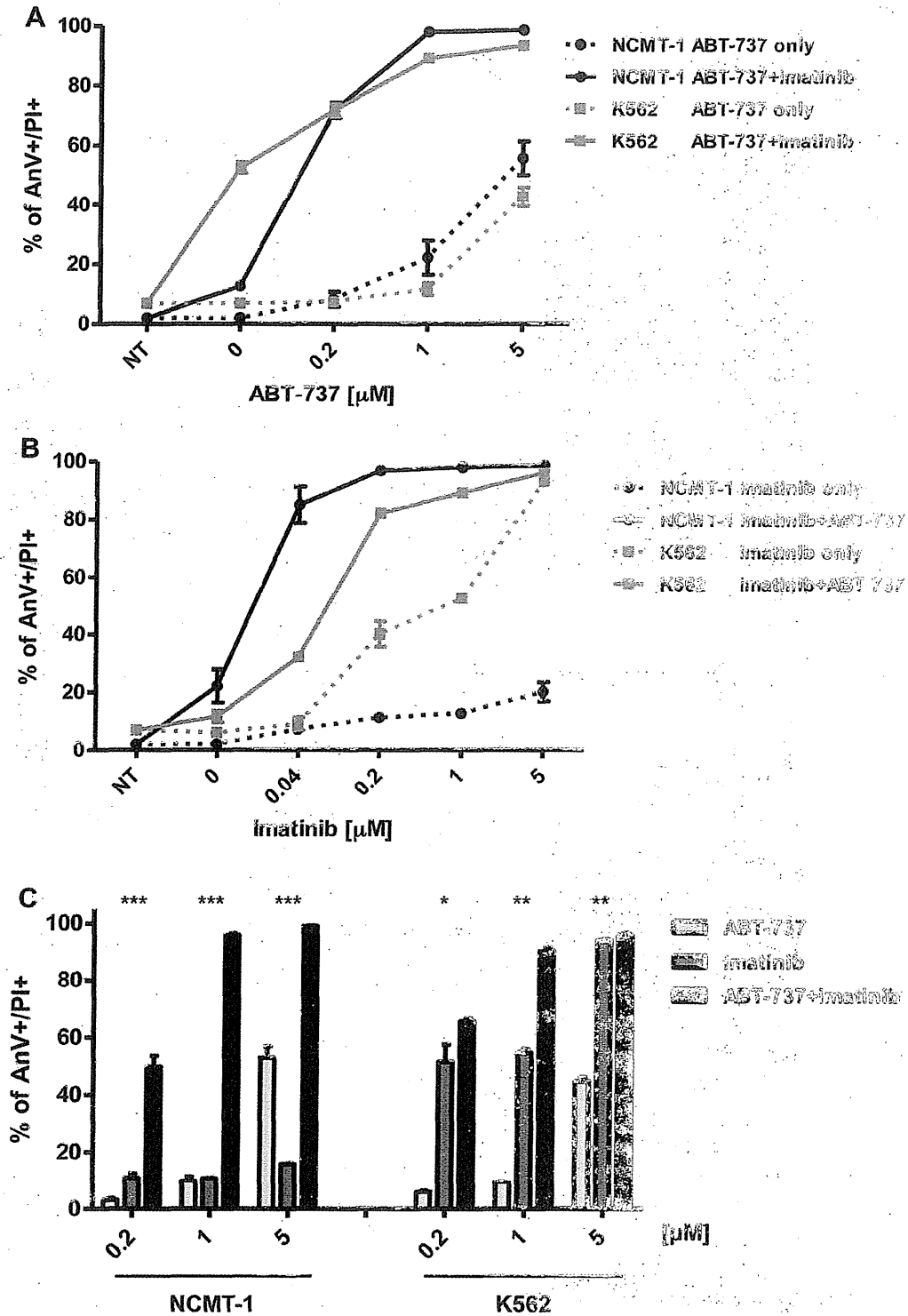

Figure 4. The resistance to TKI in NCMT-1 cells is overcome by the BH3-mimetic, ABT-737. NCMT-1 or K562 cells were treated with combinations of imatinib, ABT-737, or both for 48 h, before analysis of cell death using flow cytometric Annexin V-FITC/PI assays. (**A**) Cell death observed using various concentrations of ABT-737 with or without a constant dose of 1 μM imatinib. (**B**) Cell death observed using various concentrations of imatinib with or without a constant dose of 1 μM ABT-737. (**C**) Cell death observed using equal concentrations of imatinib and ABT-737 over a range of doses (0.2, 1, 5 μM). At each dose, the combination of imatinib and ABT-737 produced a significant synergistic effect in both cell lines. Synergistic effects were calculated by CalcuSyn software. Asterisks indicate the combination index (CI) of each dose as follows; $*5 \times 10^{-2}$–5×10^{-7}, $**5 \times 10^{-7}$–5×10^{-12}, $***<5 \times 10^{-12}$. Each point represents the mean value taken from three independent experiments with error bars indicating standard error of mean.

Table 1. Combination index

Cell line	Combination (μM)		Combination index
	Imatinib	ABT-737	
K562	0.2	0.2	0.004
	1	1	4.70E-07
	5	5	4.58E-09
NCMT-1	0.2	0.2	2.28E-12
	1	1	6.94E-27
	5	5	5.55E-33

To examine whether t(3;12) was maintained in the cell line, we performed fluorescence in situ hybridization analysis using 5′ (red) and 3′ (green) TEL probes. This analysis showed divided 5′ and 3′ probes indicating that the *TEL* translocation observed in the patient cells was maintained in the cell line (Fig. 1C, right panel).

Previous reports revealed that the *TEL/MDS1/EVI1* fusion gene was constructed from the fusion between Exon 2 of *TEL*, *MDS1*, and Exon 2 of *EVI1* as the break points [33]. To confirm the existence of the *TEL/EVI1* fusion in NCMT-1 cells, we performed reverse transcriptase PCR using *TEL*- and *EVI1*-specific primers. This analysis indicated high expression of the *TEL/EVI1* fusion in NCMT-1 (Fig. 1D, top panel), but not control (K562 or SU-DHL4) cells. Furthermore, reverse transcriptase PCR using *EVI1*-specific primers directed to the sequence upstream of the expected break point and to Exon 3 indicated weak expression of wild-type *EVI1* in NCMT-1 and K562 cells (Fig. 1D, middle panel). Sequencing of the amplified DNA confirmed the existence of the *TEL/MDS1/EVI1* fusion, with the expected break point (Supplementary Figure E1; online only, available at www.exphem.org). Protein expression of the fusion was confirmed by immunoblotting with high expression of the MDS1/EVI1 fusion observed, alongside correspondingly lower expression of the EVI1 protein, in NCMT-1 but not K562 cells (Fig. 1E).

Partial resistance of NCMT-1 cells to TKIs

As the CML from this patient was refractory to various treatments including imatinib, we performed the MTT assay to examine whether the cell line was resistant to the TKIs imatinib and dasatinib. This indicated that both TKIs potently suppressed proliferation of K562 cells, while only partially suppressing NCMT-1 proliferation. Accordingly, for imatinib, percent of control for NCMT-1 vs K562 was 7.2% vs 35.2% at 5 μM ($p = 0.004$); for dasatinib, percent of control was 12.2% vs 36.1% at 50 nM ($p = 0.004$) (Fig. 2A, B). Cell death evaluated by the Annexin V/PI assay revealed that NCMT-1 was significantly more resistant to imatinib compared to K562 (NCMT-1; 20.2%, K562; 94.5%, at 5 μM imatinib; $p < 0.0001$) (Fig. 2C). Cell cycle analysis after imatinib treatment revealed a clear population of sub-G_1, apoptotic cells in the K562 cell line, with very few sub-G_1 cells induced in the NCMT-1 cell line. However, profound G_1-arrest was observed in NCMT-1 cells, indicating that BCR-ABL is a key driver of proliferation for these cells and that they retain sensitive to inhibition by the drug, but that they possess an additional anti-apoptotic regulator compared to K562 cells (Fig. 2D, E).

Downstream signaling from BCR-ABL is correctly transduced in NCMT-1 cells

As detailed here, acquired resistance to imatinib can result from several sources. To determine the basis of resistance in NCMT-1 cells, we first analyzed the sequence of *BCR-ABL* in these cells and confirmed that no mutations were present in the gene (data not shown). To confirm that resistance was not due to overexpression of BCR-ABL, we performed immunoblotting and showed that the expression of BCR-ABL in resistant (NCMT-1) vs sensitive (K562) cells was equivalent (Fig. 3A, top panel).

Subsequently, to confirm whether the anticipated downstream intracellular signals from *BCR-ABL* were transduced in NCMT-1 cells and blocked by the TKI, we performed further immunoblotting. As shown in Figure 3A, phosphorylation of BCR-ABL was markedly reduced in the presence of imatinib and dasatinib in both K562 and NCMT-1 cells. Further markers of downstream signaling (phosphorylated CrkL and signal transducers and activators of transcription 5) were also suppressed in the presence of imatinib and dasatinib in NCMT-1 and K562 cells. Taken together, we conclude that the immediate downstream signaling from BCR-ABL is typical in NCMT-1 cells, and broadly similar to that seen in TKI-sensitive K562 cells. As the immediate downstream signaling was normal in NCMT-1 cells, we subsequently analyzed the apoptosis-related proteins in NCMT-1 and K562 cells before and after TKI treatment.

We previously demonstrated that the induction of apoptosis in CML cells after imatinib treatment is regulated by the members of the BCL-2 family and we examined the expression of these proteins [34]. In NCMT-1 cells, the pro-apoptotic BH3-only protein BIM was apparently suppressed and not strongly upregulated in the presence of imatinib or dasatinib, in contrast to K562 cells (Fig. 3B and [34]). Furthermore, the pro-survival protein, BCL-2 was strongly expressed in NCMT-1 cells and absent in K562 cells. The expression of other pro-survival proteins, including BCL-xL and MCL-1, were broadly similar in both NCMT-1 and K562 cells (Fig. 3B and data not shown).

ABT-737 resensitizes NCMT-1 cells to imatinib

ABT-737 is a BH3-mimetic that inhibits the function of a subset of the pro-survival proteins (BCL-2, BCL-xL, and BCL-w) and, as a single agent, can lead to apoptosis of tumor cells dependent on these pro-survival molecules [35]. Previous reports suggest that ABT-737 can play an important role in overcoming resistance to TKI [34], thus we analyzed the ability of ABT-737 to resensitize NCMT-1

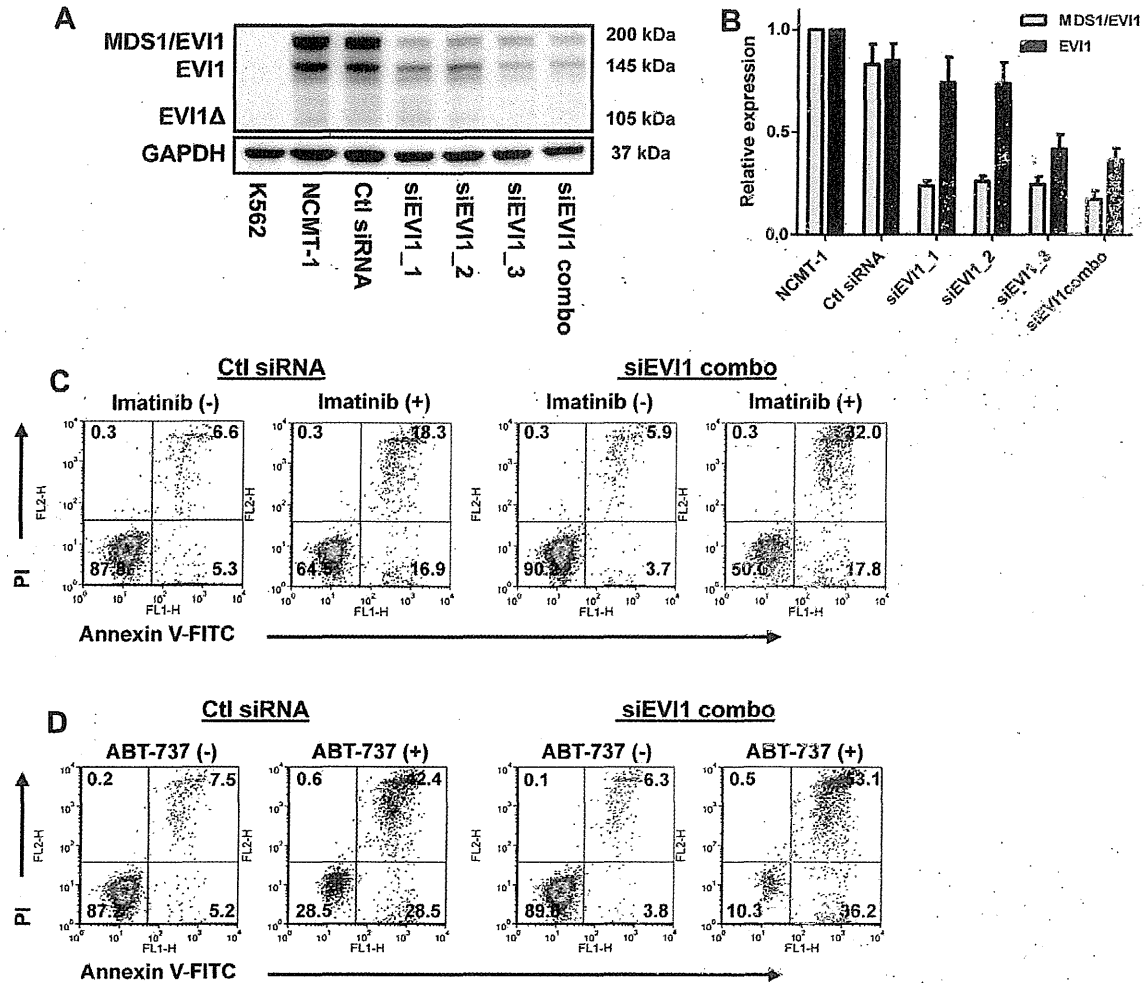

Figure 5. MDS1/EVI1 and EVI1 knockdown results in the suppression of phosphorylated-BAD via the AKT pathway, and partially restores the sensitivity to imatinib in NCMT-1 cells. (**A**) Whole cell lysates were obtained 48 h after nucleofection of NCMT-1 cells with the siRNA indicated. Immunoblotting for MDS1/EVI1 and glyceraldehyde phosphate dehydrogenase (GAPDH) as a loading control was then performed. (**B**) Densitometry analysis of MDS1/EVI1 and EVI1 expression normalized to GAPDH was performed. Each point represents of mean value taken from six independent experiments, with error bars indicating standard error of mean. (**C, D, E, F**) Sensitivity of siEVI1-transfected NCMT-1 cells to imatinib and ABT-737. NCMT-1 cells nucleofected with the siRNA indicated were rested for 48 h before addition of 5 μM imatinib (**C**) or 5 μM ABT-737 (**D**) for 48 h and assessment of cell death performed as in Figure 4. These data indicate the partial restoration of sensitivity to imatinib (**C**) and ABT-737 (**D**) in NCMT-1 cells transfected with siEVI1 compared to control siRNA.

cells to imatinib. In the presence of various concentrations of ABT-737 ± a constant dose of imatinib (1 μM), we performed cell death assays on NCMT-1 and K562 cells. In the presence of imatinib alone, we observed that NCMT-1 cells were resistant and K562 cells sensitive, as before. However, the cell death induced by imatinib was clearly increased in the presence of ABT-737 in both cell lines (Fig. 4A) with as little as 0.2 μM ABT-737, resulting in death of 70% to 80% of the cells. In the reciprocal experiment, varying the level of imatinib in the presence of a constant (1 μM) ABT-737, cell death was again clearly increased, especially in the NCMT-1 cells at extremely low doses (0.04 μM) of imatinib (Fig. 4B). To more formally evaluate the synergistic effect of imatinib combined with ABT-737, we analyzed cell death in the presence of equivalent concentrations of both drugs. As shown in Table 1, significant synergy, indicated by a combination index of <1, was observed at all three concentrations of drugs assessed (0.2, 1, and 5 μM) in NCMT-1 and K562 cells, however, the combination index was much lower, indicative of stronger synergy, in NCMT-1 rather than K562 cells (Fig. 4C). These data clearly indicate that ABT-737 can potently overcome the resistance of NCMT-1 cells to imatinib.

MDS1/EVI1 overexpression is associated with resistance to imatinib in NCMT-1 cells

To uncover whether the MDS1/EVI1 fusion was associated with the observed resistance to imatinib, we analyzed its

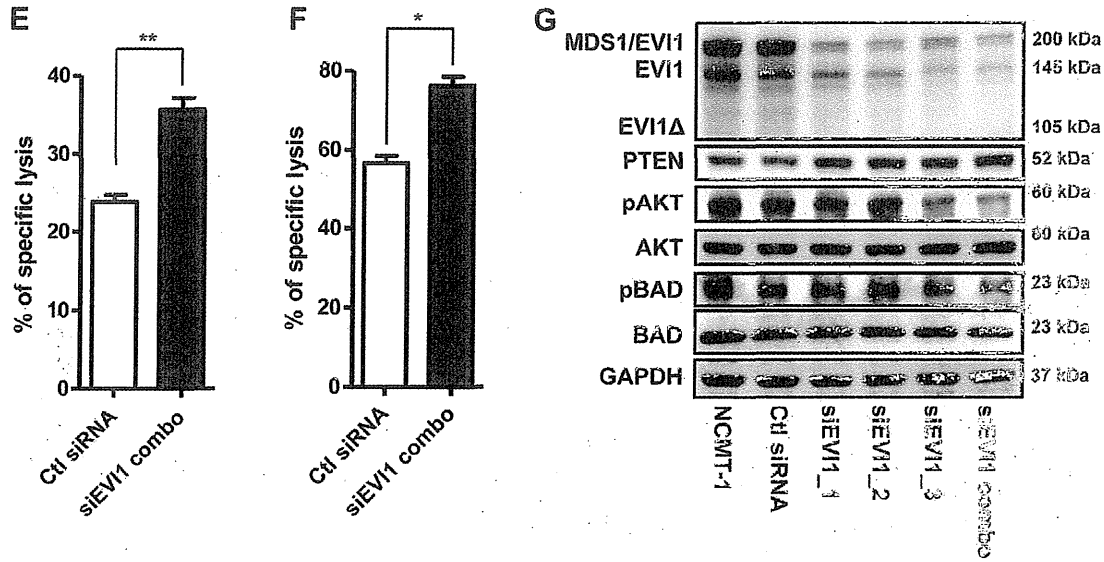

Figure 5. (*Continued*) Results are shown as representative dot plots from three to four independent experiments and are summarized in (**E**) and (**F**). Each point represents the mean value taken from two to three independent experiments, with error bars indicating the SEM. Asterisks indicate the *p* value as follows; *0.05, **0.005. (**G**) Whole cell lysates were obtained 48 h after nucleofection of NCMT-1 cells with the siRNA indicated. Immunoblotting for MDS1/EVI1, PTEN, AKT, pAKT, pBAD, BAD, and GAPDH as a loading control was then performed. Analysis of siEVI1-transfected NCMT-1 cells revealed the upregulation of PTEN and the downregulation of pAKT and pBAD (pSerine 136). All of the images except that relating to pBAD and BAD were derived from the same membrane. The pBAD and BAD blot was taken from a separate membrane using the same cell lysate.

role in NCMT-1 cells by reducing its expression using a panel of EVI1-specific siRNAs (siEVI1). Using three different siEVI1, alone and in combination (combo; where each was added in a one-third dose), we nucleofected NCMT-1 cells and confirmed the suppression of both the MDS1/EVI1 fusion and, to a lesser extent, the EVI1 protein by immunoblotting (Fig. 5A, B). We subsequently assessed the sensitivity of these cells to imatinib treatment. Cell death assays indicated that reduction in MDS1/EVI1 and EVI1 expression by the siEVI1 produced a partial but robust and statistically significant ($p = 0.003$) restoration of sensitivity to imatinib compared to the control siRNA-transfected NCMT-1 cells (Fig. 5C, E). Furthermore, the sensitivity to ABT-737 was increased in siEVI1-transfected cells compared to control siRNA-transfected cells ($p = 0.02$) (Fig. 5D, F). Taken together, these data indicate that overexpression of the MDS1/EVI1 fusion (and potentially the EVI1 protein) in NCMT-1 cells is associated with the resistance to imatinib and sensitivity to ABT-737 by suppressing apoptosis.

Concurrently, we analyzed whether the effect of siRNA might be related to changes in the BCL-2 family members. Given the relatively high expression of BCL-2 and low expression of BIM in NCMT-1 cells (in comparison to K562 cells), we first considered whether MDS1/EVI1 might regulate these proteins. However, in siEVI1-transfected NCMT-1 cells, both BIM and BCL-2 were unchanged (Supplementary Figure E2; online only, available at www.exphem.org), indicating that the MDS1/EVI1 fusion does not regulate these proteins. Moreover, the expression of BCL-xL and MCL-1 also remained unaffected by siEVI1 transfection (Supplementary Figure E2; online only, available at www.exphem.org). As a recent report revealed that EVI1 repressed PTEN expression and activated AKT [36], we analyzed the AKT pathway in the siEVI1-transfected NCMT-1 cells. In these cells, the level of PTEN was increased and that of phosphorylated AKT (pAKT) was clearly decreased compared to untreated cells or control-transfected cells, although the total level of AKT remained unchanged (Fig. 5G). To confirm this observation and also potentially reveal a direct pathway toward apoptotic regulation, we subsequently probed the phosphorylation status of the pro-apoptotic BH3-only protein BAD, a known substrate of AKT, using phosphospecific antibodies. As anticipated, the extent of phospho-BAD was suppressed in siEVI1-transfected NCMT-1 cells (Fig. 5G). Taken together, these data indicate that overexpression of MDS1/EVI1 is associated with resistance to imatinib (and dasatinib) through the inhibition of apoptosis via AKT and its downstream substrate BAD (Figs. 5G and 6D).

AKT as a potential therapeutic target for EVI1-expressing tumors

As pAKT is upregulated in NCMT-1 cells and suppressed by the downregulation of EVI1, we investigated whether AKT inhibition is a potential therapeutic target for EVI1-positive tumors. In the presence of 50 μM AKT inhibitor (AKTi) alone, very little cell death was observed. Similarly, when up to 25 μM AKTi was combined with low (0.2 μM) or

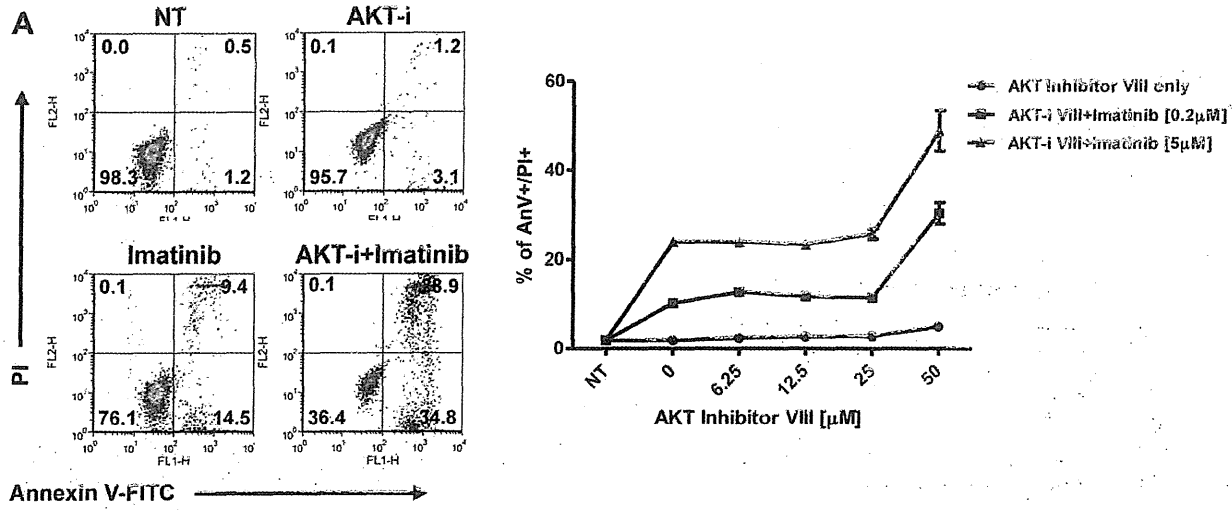

Figure 6. The resistance to TKI in NCMT-1 cells is overcome by the inhibition of AKT. NCMT-1 cells were treated with combinations of imatinib, AKT inhibitor (AKT-i), or both for 48 h, before analysis of cell death as in Figure 4. (**A**) Cell death observed using various concentrations of AKT-i with or without a constant dose of 0.2 or 5 μM imatinib. The representative dot plots of no treatment (NT), 5 μM imatinib alone, 50 μM AKT-i alone, and combination of these two were indicated. Each point represents the mean value taken from three independent experiments, with error bars indicating the standard error of mean (SEM).

high (5 μM) doses of imatinib, cell death was not increased compared to drugs alone. However, in the presence of 50 μM AKTi, cell death was clearly increased when combined with both high and low doses of imatinib (Fig. 6A). In the reverse experiment, varying doses of imatinib in the presence of a constant dose (50 μM) of AKTi, cell death was again increased in the presence of imatinib compared to imatinib alone (Fig. 6B). To confirm that these combination effects were specific for the inhibition of AKT, we investigated the phosphorylation status of AKT in the presence of varying doses of the AKTi. As expected, the phosphorylation status of AKT decreased substantially when the dose of inhibitor was increased from 25 μM to 50 μM, in keeping with the biological effects at these doses, but the total level of AKT remained unchanged (Fig. 6C). Further confirming the close association between the activation status of AKT and BAD, inhibition of pAKT correlated with a reduction in pBAD levels after treatment with the AKT inhibitor. Taken together, these data indicate that inhibition of pAKT resensitizes NCMT-1 cells to death with TKI. This effect mimics that seen following inactivation of EVI1, which indicates that targeting AKT could be a promising therapeutic strategy for treating EVI1-expressing tumors (Fig. 6D).

Discussion

Here, we have detailed the establishment of a novel, CML cell line, NCMT-1, which displays partial resistance to TKI, reflecting the clinical response of the patient from whom it was derived. Both the primary tumor and derived NCMT-1 cell line express the TEL/MDS1/EVI1 fusion protein derived from the t(3;12)(q26;p13) chromosomal abnormality. Our subsequent experiments revealed that overexpression of MDS1/EVI1 results in the inhibition of the pro-apoptotic protein, BAD, through effects on the AKT pathway. Addition of the BH3-mimetic, ABT-737, could overcome the resistance of the NCMT-1 cells to TKI and the combination of TKI + ABT-737 was highly synergistic in NCMT-1 as well as TKI-sensitive K562 cells. Finally, the combination of TKI + AKTi was also shown to resensitize NCMT-1 cells to apoptosis, indicating that AKT is a promising target for treating EVI1-positive malignancies.

Resistance to TKI in CML encompasses the BCR-ABL–dependent and –independent mechanisms detailed here [9]. In NCMT-1, no mutation of the BCR-ABL kinase domain was observed, and expression of BCR-ABL was shown by immunoblotting to be equivalent to that in the TKI-sensitive cell line K562. In addition, the immediate downstream signaling from BCR-ABL appeared similar to that seen in K562 cells, and sensitive to inhibition by imatinib, indicating a BCR-ABL–independent cause of resistance in NCMT-1 cells. The likely cause of the resistance in NCMT-1 is via an impact of MDS1/EVI1 on the BCL-2 family of apoptotic proteins. Furthermore, as ABT-737 combined with TKI could overcome the observed resistance to TKI, this indicates that the resistance was due to a downstream regulator of apoptosis, likely related to one or more BCL-2 family members known to be regulated by ABT-737 [37].

The patient from whose CML cells the NCMT-1 cell line was developed, presented in blast crisis and possessed the relatively rare chromosomal abnormality, t(3;12)(q26;p13) [22]. We observed the existence of this chromosomal aberration and also a relatively high expression of BCL-2 in the NCMT-1 cells and hypothesized that they were related to

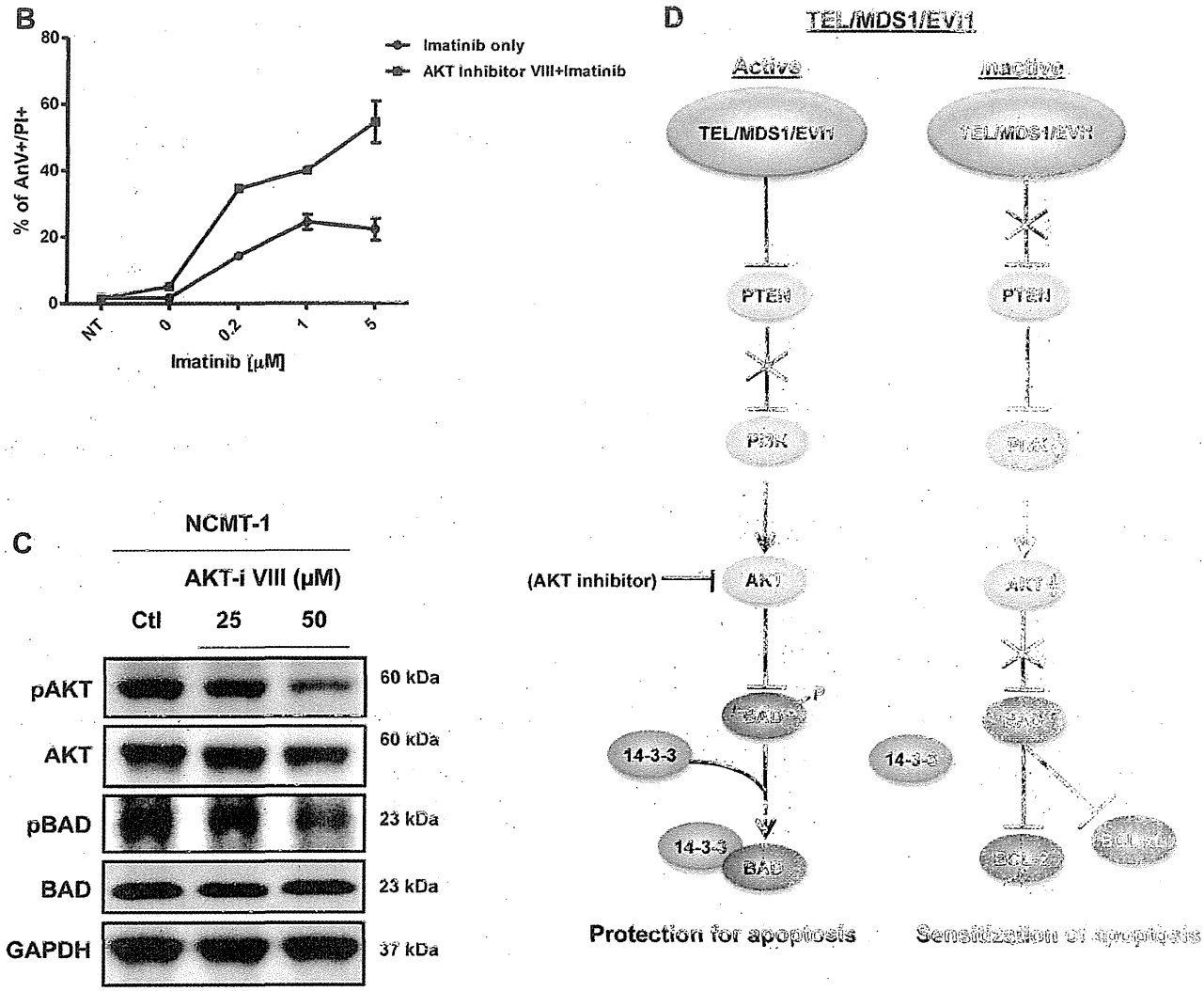

Figure 6. (*Continued*) (**B**) Cell death observed using various concentrations of imatinib with or without a constant dose of 50 μM AKT-i. Each point represents the mean value taken from three independent experiments, with error bars indicating the SEM. (**C**) Whole cell lysates were obtained 48 h after incubation with the AKT-i at various doses (0, 25, 50 μM). Immunoblotting for AKT, pAKT, BAD, pBAD, and glyceraldehyde phosphate dehydrogenase (GAPDH) as a loading control was then performed. (**D**) Schema representing the proposed downstream signaling pathway transduced by TEL/MDS1/EVI1. When TEL/MDS1/EVI1 is active, it suppresses PTEN resulting in activation of PI3K/AKT. Active, phosphorylated AKT leads to the phosphorylation of BAD, resulting in its binding to 14-3-3 protein, suppressing its pro-apoptotic activity. Conversely, when TEL/MDS1/EVI1 is not expressed or inactivated, PTEN suppresses the PI3K/AKT pathway. Reduced phosphorylation of BAD allows liberation from the 14-3-3 complex, augmenting its ability to counteract the protective functions of BCL-2 and BCL-xL, leading to sensitization of apoptosis. Inhibition of AKT mimics inactivation of EVI1.

disease progression in blast crisis. Using *EVI1*-specific siRNA, we were able to demonstrate that MDS1/EVI1 does not regulate BCL-2 (or BIM) expression in NCMT-1 cells, indicating an alternative mechanism. Previous reports suggest that overexpression of LYN can result in BCL-2 expression, however, in that report, LYN inhibited the immediate signaling pathway downstream of BCR-ABL, including effects on signal transducers and activators of transcription 5, which were not seen here [13]. Therefore, it seems likely that BCL-2 expression in NCMT-1 cells is regulated by an alternative route, independent of LYN and MDS1/EVI1.

ABT-737 displayed a significant synergistic effect in killing NCMT-1 and K562 cells when combined with TKI. Although ABT-737 is not suitable for clinical practice due to poor physiochemical and pharmaceutical properties [38], the closely related Navitoclax (ABT-263), which is orally bioavailable, is in clinical development [37,39]. ABT-263 is already demonstrating promising results in lymphoid and other malignancies, providing optimism that these reagents will rapidly become clinically available for combination studies [40,41]. In NCMT-1 cells, the potent effects of the TKI + ABT-737 combination might be due to its relatively high expression of BCL-2. However,

it should be noted that ABT-737 alone had very limited effects, indicating that overcoming high levels of BCL-2 alone is insufficient to cause efficient cell death. The fact that this potent synergy was also observed in K562 cells, which are sensitive to TKI, and that BCL-2 and BCL-xL (which are the main targets of ABT-737 and ABT-263), are frequently overexpressed in advanced stage of CML [1,17], indicates that this combination would be beneficial in various stages of CML progression to improve clinical outcome. Furthermore, the fact that the synergistic effect was observed with low concentrations of both drugs might also indicate an advantage in terms of reducing drug usage to improve safety and efficacy, although clearly further investigation is warranted.

The molecular consequence of the TEL/MDS1/EVI1 fusion has not been fully resolved to date, probably due to its relative rarity [22]. As observed in the NCMT-1 cells, break points of the fusion are located on Exon 2 of *TEL*, *MDS1* and Exon 2 of *EVI1*, thus the ETS domain and DNA binding site of the TEL gene are absent in the fusion gene [42]. In contrast, the fusion gene does contain the two zinc finger motifs of the *EVI1* gene, and so the function of the *TEL/MDS1/EVI1* fusion likely reflects that of *EVI1* [43]. The siEVI1s suppressed the MDS1/EVI1 fusion to a greater extent than the EVI1 protein. Our data indicate that the overexpression of MDS1/EVI1 is able to regulate the phosphorylation status, and thereby likely the activity of AKT, which is coincident with a recent report that indicates EVI1 represses PTEN and activates the phosphoinositide 3-kinase/AKT pathway [36]. Interestingly, although the MDS1/EVI1 fusion was expressed at a far higher level than the EVI1 protein, and we observed a greater effect of the siRNA on reducing its expression a recent report indicated that EVI1 expression was more relevant to clinical outcome compared to MDS1/EVI1 expression [18]. Therefore, it remains possible that the effects we observed were related to reduction in EVI1 expression. Unfortunately, we are currently unable to modulate the expression of these two proteins differentially. Irrespective, the hypothesis that follows is that targeting AKT could be a rational treatment strategy for EVI1-positive tumors. Several AKT inhibitors are in development and/or currently undergoing clinical investigation [44], making this a realistic ambition. Furthermore, considering the increased frequency of this aberration following TKI treatment [45], additional investigation of this transcription factor and its related fusion proteins is warranted, particularly in terms of their regulation of apoptosis and the potential sensitization with ABT-737 or AKTi.

Our findings, although derived from a single cell line, have clear relevance in terms of the molecular basis of disease progression and BCR/ABL-independent TKI resistance in CML and the function of dysregulated EVI1 in tumor cells. In particular, the association of the overexpression of MDS1/EVI1 with the regulation of apoptosis has not been previously appreciated, and our findings that these proteins suppress the function of BAD via the AKT pathway and targeting phosphorylated AKT mimics the inhibition of EVI1 are novel. Furthermore, advanced-stage CML is currently largely intractable, and our findings that BH3-mimetics synergize with TKI, even in TKI-insensitive cells, warrant further evaluation, including clinically, in the near future.

Funding disclosure

The authors gratefully acknowledge the Daiichi-Sankyo Foundation for Life Sciences for a grant to K.S., Grant-Aid for Scientific Research (B) 22390192 and a Health Labour Sciences Research Grant H22YE010-01 for T.N., and the Association for International Cancer Research (AICR) for a grant to M.S.C. and C.K.H.

Acknowledgments

We would like to thank Dr. Ryohei Tanizaki for assistance with cell-line establishment, Kunihiko Takeyama, M.D., Ph.D. (Dana-Faber Cancer Institute, Boston, MA, USA) for providing the SU-DHL4 cell line, Kiyosumi Shibata, M.D., Ph.D. for providing the SK-OV3 cell line, Yoshitsugu Koyama, M.D. and Hiroshi Kosugi, M.D., Ph.D. (Ogaki Municipal Hospital, Ogaki, Japan) and Akio Kohno M.D., Ph.D. (JA Aichi Konan Kosei Hospital, Konan, Japan) for providing samples and information relating to this patient and Dr. A Hayden for assistance with synergy calculations.

Author contributions: K.S., A.T., Y.M., M.S.C., and T.N. designed research and analyzed results. K.S. and C.K.H. performed experiments. A.A. established the cell line. K.S. and M.S.C. wrote the manuscript. A.T., Y.M., and T.N. edited the manuscript. H.K., M.S.C., and T.N. supervised research. All the authors approved the final version of manuscript.

Conflict of interest disclosure

No financial interest/relationships with financial interest relating to the topic of this article have been declared.

References

1. Melo JV, Barnes DJ. Chronic myeloid leukaemia as a model of disease evolution in human cancer. Nat Rev Cancer. 2007;7:441–453.
2. Sawyers CL, McLaughlin J, Witte ON. Genetic requirement for Ras in the transformation of fibroblasts and hematopoietic cells by the Bcr-Abl oncogene. J Exp Med. 1995;181:307–313.
3. Skorski T, Kanakaraj P, Nieborowska-Skorska M, et al. Phosphatidylinositol-3 kinase activity is regulated by BCR/ABL and is required for the growth of Philadelphia chromosome-positive cells. Blood. 1995;86:726–736.
4. Druker BJ, Sawyers CL, Kantarjian H, et al. Activity of a specific inhibitor of the BCR-ABL tyrosine kinase in the blast crisis of chronic myeloid leukemia and acute lymphoblastic leukemia with the Philadelphia chromosome. N Engl J Med. 2001;344:1038–1042.
5. Kantarjian H, Giles F, Wunderle L, et al. Nilotinib in imatinib-resistant CML and Philadelphia chromosome-positive ALL. N Engl J Med. 2006;354:2542–2551.
6. Talpaz M, Shah NP, Kantarjian H, et al. Dasatinib in imatinib-resistant Philadelphia chromosome-positive leukemias. N Engl J Med. 2006; 354:2531–2541.

7. O'Brien SG, Guilhot F, Larson RA, et al. Imatinib compared with interferon and low-dose cytarabine for newly diagnosed chronic-phase chronic myeloid leukemia. N Engl J Med. 2003;348:994–1004.
8. Horowitz MM, Rowlings PA, Passweg JR. Allogeneic bone marrow transplantation for CML: a report from the International Bone Marrow Transplant Registry. Bone Marrow Transplant. 1996;17(suppl 3):S5–S6.
9. Diamond JM, Melo JV. Mechanisms of resistance to BCR-ABL kinase inhibitors. Leuk Lymphoma. 2011;52(suppl 1):12–22.
10. Apperley JF. Part I: mechanisms of resistance to imatinib in chronic myeloid leukaemia. Lancet Oncol. 2007;8:1018–1029.
11. Widmer N, Colombo S, Buclin T, Decosterd LA. Functional consequence of MDR1 expression on imatinib intracellular concentrations. Blood. 2003;102:1142.
12. Mahon FX, Belloc F, Lagarde V, et al. MDR1 gene overexpression confers resistance to imatinib mesylate in leukemia cell line models. Blood. 2003;101:2368–2373.
13. Dai Y, Rahmani M, Corey SJ, Dent P, Grant S. A Bcr/Abl-independent, Lyn-dependent form of imatinib mesylate (STI-571) resistance is associated with altered expression of Bcl-2. J Biol Chem. 2004;279:34227–34239.
14. Donato NJ, Wu JY, Stapley J, et al. BCR-ABL independence and LYN kinase overexpression in chronic myelogenous leukemia cells selected for resistance to STI571. Blood. 2003;101:690–698.
15. Holyoake T, Jiang X, Eaves C, Eaves A. Isolation of a highly quiescent subpopulation of primitive leukemic cells in chronic myeloid leukemia. Blood. 1999;94:2056–2064.
16. Holyoake TL, Jiang X, Jorgensen HG, et al. Primitive quiescent leukemic cells from patients with chronic myeloid leukemia spontaneously initiate factor-independent growth in vitro in association with up-regulation of expression of interleukin-3. Blood. 2001;97:720–728.
17. Radich JP. The biology of CML blast crisis. Hematology Am Soc Hematol Educ Program. 2007;384–391.
18. Barjesteh van Waalwijk van Doorn-Khosrovani S, Erpelinck C, van Putten WL, et al. High EVI1 expression predicts poor survival in acute myeloid leukemia: a study of 319 de novo AML patients. Blood. 2003; 101:837–845.
19. Mitani K, Ogawa S, Tanaka T, et al. Generation of the AML1-EVI-1 fusion gene in the t(3;21)(q26;q22) causes blastic crisis in chronic myelocytic leukemia. EMBO J. 1994;13:504–510.
20. Ogawa S, Kurokawa M, Mitani K, Yazaki Y, Hirai H. Overexpression of Evi-1 and dysmegakaryopoiesis in human leukemias: reply to Carapeti, Goldman and Cross, Leukemia 1996;10:1561. Leukemia. 1996;10:1849.
21. Suzukawa K, Parganas E, Gajjar A, et al. Identification of a breakpoint cluster region 3' of the ribophorin I gene at 3q21 associated with the transcriptional activation of the EVI1 gene in acute myelogenous leukemias with inv(3)(q21q26). Blood. 1994;84:2681–2688.
22. Nakamura Y, Nakazato H, Sato Y, Furusawa S, Mitani K. Expression of the TEL/EVI1 fusion transcript in a patient with chronic myelogenous leukemia with t(3;12)(q26;p13). Am J Hematol. 2002;69:80–82.
23. Goyama S, Yamamoto G, Shimabe M, et al. Evi-1 is a critical regulator for hematopoietic stem cells and transformed leukemic cells. Cell Stem Cell. 2008;3:207–220.
24. Kurokawa M, Mitani K, Irie K, et al. The oncoprotein Evi-1 represses TGF-beta signalling by inhibiting Smad3. Nature. 1998;394:92–96.
25. Kurokawa M, Mitani K, Yamagata T, et al. The evi-1 oncoprotein inhibits c-Jun N-terminal kinase and prevents stress-induced cell death. EMBO J. 2000;19:2958–2968.
26. Tanaka T, Nishida J, Mitani K, Ogawa S, Yazaki Y, Hirai H. Evi-1 raises AP-1 activity and stimulates c-fos promoter transactivation with dependence on the second zinc finger domain. J Biol Chem. 1994; 269:24020–24026.
27. Baccarani M, Cortes J, Pane F, et al. Chronic myeloid leukemia: an update of concepts and management recommendations of European LeukemiaNet. J Clin Oncol. 2009;27:6041–6051.
28. Atsumi A, Tomita A, Kiyoi H, Naoe T. Histone deacetylase 3 (HDAC3) is recruited to target promoters by PML-RARalpha as a component of the N-CoR co-repressor complex to repress transcription in vivo. Biochem Biophys Res Commun. 2006;345:1471–1480.
29. Chan HT, Hughes D, French RR, et al. CD20-induced lymphoma cell death is independent of both caspases and its redistribution into triton X-100 insoluble membrane rafts. Cancer Res. 2003;63:5480–5489.
30. Minami Y, Kiyoi H, Yamamoto Y, et al. Selective apoptosis of tandemly duplicated FLT3-transformed leukemia cells by Hsp90 inhibitors. Leukemia. 2002;16:1535–1540.
31. Cragg MS, Howatt WJ, Bloodworth L, Anderson VA, Morgan BP, Glennie MJ. Complement mediated cell death is associated with DNA fragmentation. Cell Death Differ. 2000;7:48–58.
32. Hiraga J, Tomita A, Sugimoto T, et al. Down-regulation of CD20 expression in B-cell lymphoma cells after treatment with rituximab-containing combination chemotherapies: its prevalence and clinical significance. Blood. 2009;113:4885–4893.
33. Peeters P, Wlodarska I, Baens M, et al. Fusion of ETV6 to MDS1/EVI1 as a result of t(3;12)(q26;p13) in myeloproliferative disorders. Cancer Res. 1997;57:564–569.
34. Kuroda J, Puthalakath H, Cragg MS, et al. Bim and Bad mediate imatinib-induced killing of Bcr/Abl+ leukemic cells, and resistance due to their loss is overcome by a BH3 mimetic. Proc Natl Acad Sci U S A. 2006;103:14907–14912.
35. Oltersdorf T, Elmore SW, Shoemaker AR, et al. An inhibitor of Bcl-2 family proteins induces regression of solid tumours. Nature. 2005;435: 677–681.
36. Yoshimi A, Goyama S, Watanabe-Okochi N, et al. Evi1 represses PTEN expression and activates PI3K/AKT/mTOR via interactions with polycomb proteins. Blood. 2011;117:3617–3628.
37. Cragg MS, Harris C, Strasser A, Scott CL. Unleashing the power of inhibitors of oncogenic kinases through BH3 mimetics. Nat Rev Cancer. 2009;9:321–326.
38. Vogler M, Dinsdale D, Dyer MJ, Cohen GM. Bcl-2 inhibitors: small molecules with a big impact on cancer therapy. Cell Death Differ. 2009;16:360–367.
39. Tse C, Shoemaker AR, Adickes J, et al. ABT-263: a potent and orally bioavailable Bcl-2 family inhibitor. Cancer Res. 2008;68:3421–3428.
40. Wilson WH, O'Connor OA, Czuczman MS, et al. Navitoclax, a targeted high-affinity inhibitor of BCL-2, in lymphoid malignancies: a phase 1 dose-escalation study of safety, pharmacokinetics, pharmacodynamics, and antitumour activity. Lancet Oncol. 2010;11:1149–1159.
41. Gandhi L, Camidge DR, Ribeiro de Oliveira M, et al. Phase I study of Navitoclax (ABT-263), a novel Bcl-2 family inhibitor, in patients with small-cell lung cancer and other solid tumors. J Clin Oncol. 2011;29: 909–916.
42. Bohlander SK. ETV6: a versatile player in leukemogenesis. Semin Cancer Biol. 2005;15:162–174.
43. Goyama S, Kurokawa M. Pathogenetic significance of ecotropic viral integration site-1 in hematological malignancies. Cancer Sci. 2009; 100:990–995.
44. Hirai H, Sootome H, Nakatsuru Y, et al. MK-2206, an allosteric Akt inhibitor, enhances antitumor efficacy by standard chemotherapeutic agents or molecular targeted drugs in vitro and in vivo. Mol Cancer Ther. 2010;9:1956–1967.
45. Paquette RL, Nicoll J, Chalukya M, et al. Frequent EVI1 translocations in myeloid blast crisis CML that evolves through tyrosine kinase inhibitors. Cancer Genet. 2011;204:392–397.

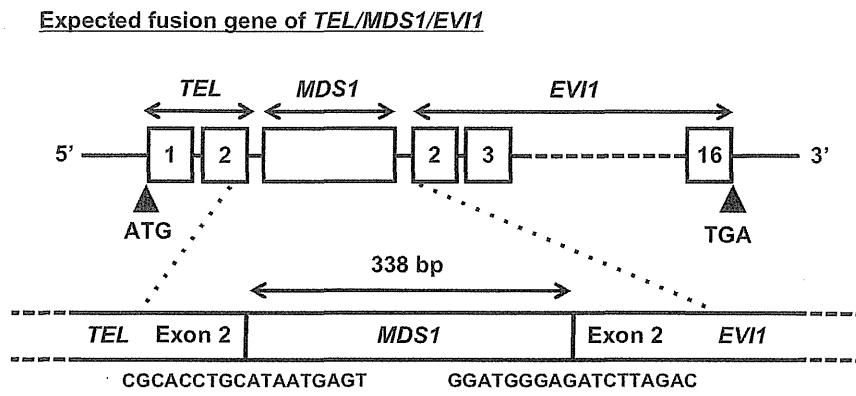

Supplementary Figure E1. Structure of the *TEL/MDS1/EVI1* fusion. A schematic representation of the *TEL/MDS1/EVI1* fusion present in the NCMT-1 cells is shown. Sequencing analysis revealed the break points of the fusion to be between Exon2 of *TEL*, *MDS1* and Exon2 of *EVI1*. This structure of the fusion gene corresponds to that reported previously [33].

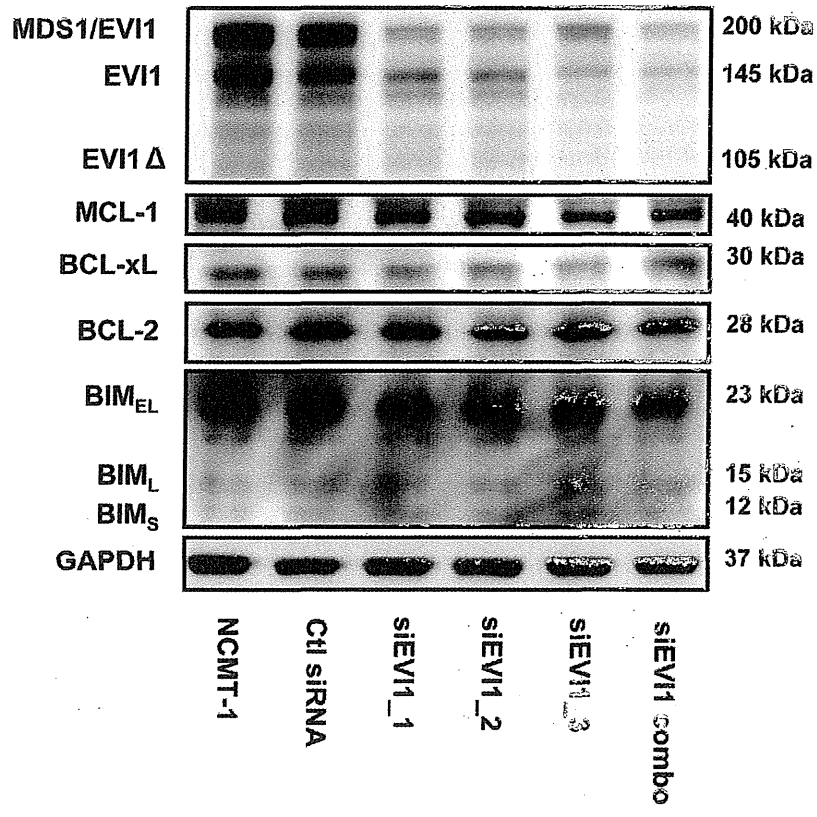

Supplementary Figure E2. MDS1/EVI1 knockdown does not affect the expression of BCL-2, BCL-xL, MCL-1, or BIM in NCMT-1 cells. Whole cell lysates were obtained 48 h after nucleofection of NCMT-1 cells with the siRNA indicated. Immunoblotting for MDS1/EVI1, BIM, BCL-2, BCL-xL, MCL-1, and glyceraldehyde phosphate dehydrogenase (GAPDH) as a loading control was then performed. BCL-2 and BIM expression were not changed by the suppression of MDS1/EVI1, indicating it does not regulate these apoptotic-related proteins. All of the images except for BCL-xL and MCL-1 were obtained from the same membrane. The BCL-xL and MCL-1 blot were taken from the same membrane.

Supplementary Table E1. Primer list

Name	Sequence	Annealing temperature (°C)	Cycles
TEL-U	5′-ATG TCT GAG ACT CCT GCT CA-3′	58	35
EVI1-U	5′-TGG AGA GCA GAT CCT AGA GA-3′	58	35
EVI1-L	5′-CAC AGT CTT CGC AGC GAT AT-3′	58	35
β-actin U	5′-TCA CTC ATG AAG ATC CTC A-3′	58	35
β-actin L	5′-TTC GTG GAT GCC ACA GGA C-3′	58	35

Supplementary Table E2. Source of primary antibodies for immunoblotting

Antibody	Source	Location
BCR-ABL (8E9)	BD Biosciences Pharmingen	San Diego, CA, USA
EVI1 (#2593)	Cell Signaling Technology (CST)	Danvers, MA, USA
pBCR-ABL (Tyr245) (#2861)	CST	Danvers, MA, USA
pCrkL (Tyr207) (#3181)	CST	Danvers, MA, USA
pSTAT5 (#9359)	CST	Danvers, MA, USA
STAT5 (#9358)	CST	Danvers, MA, USA
pERK1/2	CST	Danvers, MA, USA
ERK1/2	CST	Danvers, MA, USA
pAKT (Ser473) (#4060)	CST	Danvers, MA, USA
AKT (#9272)	CST	Danvers, MA, USA
pBAD (Ser136) (#4366)	CST	Danvers, MA, USA
BIM (#2819)	CST	Danvers, MA, USA
BIM	Enzo Life Sciences	Exeter, UK
BAD	Enzo Life Sciences	Exeter, UK
BCL-2	BD Biosciences Pharmingen	San Diego, CA, USA
BCL-2	CST	Danvers, MA, USA
BCL-xL	CST	Danvers, MA, USA
BCL-xL	BD Biosciences Pharmingen	San Diego, CA, USA
MCL-1	Abcam	Cambridge, UK
MCL-1 (#4572)	CST	Danvers, MA, USA
PTEN	Millipore	Billerica, MA, USA
GAPDH (6C5)	Abcam	Cambridge, UK

Favorable outcome of patients who have 13q deletion: a suggestion for revision of the WHO 'MDS-U' designation

Kohei Hosokawa,[1] Takamasa Katagiri,[1,2] Naomi Sugimori,[1] Ken Ishiyama,[1,3] Yumi Sasaki,[1] Yu Seiki,[1] Aiko Sato-Otsubo,[4] Masashi Sanada,[4] Seishi Ogawa,[4] and Shinji Nakao[1]

[1]Cellular Transplantation Biology, Kanazawa University Graduate School of Medical Science, Kanazawa; [2]Clinical Laboratory Science, Kanazawa University Graduate School of Medical Science, Kanazawa; [3]Tokyo Metropolitan Ohtsuka Hospital, Department of Internal Medicine, Toshima; and [4]Cancer Genomics Project, Graduate School of Medicine, University of Tokyo, Tokyo, Japan

ABSTRACT

To characterize bone marrow failure with del(13q), we reviewed clinical records of 22 bone marrow failure patients possessing del(13q) alone or del(13q) plus other abnormalities. All del(13q) patients were diagnosed with myelodysplastic syndrome-unclassified due to the absence of apparent dysplasia. Elevated glycosylphosphatidylinositol-anchored protein-deficient blood cell percentages were detected in all 16 with del(13q) alone and 3 of 6 (50%) patients with del(13q) plus other abnormalities. All 14 patients with del(13q) alone and 2 of 5 (40%) patients with del(13q) plus other abnormalities responded to immunosuppressive therapy with 10-year overall survival rates of 83% and 67%, respectively. Only 2 patients who had abnormalities in addition to the del(13q) abnormality developed acute myeloid leukemia. Given that myelodysplastic syndrome-unclassified with del(13q) is a benign bone marrow failure subset characterized by good response to immunosuppressive therapy and a high prevalence of increased glycosylphosphatidylinositol-anchored protein-deficient cells, del(13q) should not be considered an intermediate-risk chromosomal abnormality.

Key words: glycosylphosphatidylinositol-anchored protein-deficient, cells, bone marrow failure, 13q deletion, immunosuppressive therapy.

Citation: Hosokawa K, Katagiri T, Sugimori N, Ishiyama K, Sasaki Y, Seiki Y, Sato-Otsubo A, Sanada M, Ogawa S, and Nakao S. Favorable outcome of patients who have 13q deletion: a suggestion for revision of the WHO 'MDS-U' designation. Haematologica 2012;97(12):1845-1849. doi:10.3324/haematol.2011.061127

Introduction

Numerical karyotypic abnormalities such as -7/del(7q) and del(13q) are occasionally seen in patients with bone marrow (BM) failure who do not exhibit typical signs of myelodysplasia. The 2008 World Health Organization (WHO) criteria defined this subset of BM failure as myelodysplastic syndrome-unclassified (MDS-U) because patient progression to leukemia was still possible. However, no large patient study has been conducted to explore an association between del(13q) and pre-leukemia.[1] Several anecdotal reports have shown that BM failure patients with del(13q) responded to immunosuppressive therapy (IST) and had a favorable prognosis.[2,3] However, the incidence of BM failure with del(13q) and its relationship with immune pathophysiology of BM failure remain unclear.

Several studies have identified the presence of small populations of glycosylphosphatidylinositol-anchored protein-deficient (GPI-AP$^-$) blood cells as a significant factor predicting a good response to IST in patients with aplastic anemia (AA) and low-risk myelodysplastic syndromes (MDS).[4,5] Immune mechanisms are, therefore, thought to be involved in the increase in the GPI-AP$^-$ cells in this type of BM failure, though the exact mechanisms responsible for the increase in the GPI-AP$^-$cells remain unknown. Given that BM failure with del(13q) is likely to respond to IST, this type of BM failure may be associated with the presence of small populations of GPI-AP$^-$ cells. It is essential to precisely characterize BM failure with del(13q) because the present WHO definition of an intermediate-risk abnormality may lead to inappropriate treatment of potentially benign BM failure with hypomethylating agents or allogeneic stem cell transplants from unrelated donors. To address this issue, the present study analyzed clinical and genetic features of 22 BM failure patients possessing del(13q) by comparing them to BM failure patients with a normal karyotype.

Design and Methods

Study subjects

Clinical records were analyzed for 1,228 BM failure patients: 733 with aplastic anemia (AA), 495 with low-risk MDS, including 286 with refractory cytopenia with unilineage dysplasia (RCUD), 149 with

The online version of this article has a Supplementary Appendix.

Acknowledgments: the authors would like to thank Rie Ohmi and Kenichi Takemoto for excellent technical assistance, and Yasuhiko Yamamoto for excellent cell sorting technical support. We also thank the doctors who contributed patients to this study: Mitsufumi Nishio, Ryosuke Yamamura, Yoshiko Okikawa, Takeaki Tomoyose, Takuya Machida, Hiroshi Kanashima, Masahiro Manabe, Yukiyoshi Moriuchi, Takashi Nakaike, Yutaka Imamura, Kenji Shinohara, Taro Masunari, Akio Maeda, Hirokazu Okumura, Kazuyuki Shigeno, Masayuki Kikukawa, Hidemi Ogura, Tadashi Nagai, Hidetaka Niitsu and Senji Kasahara.
Funding: this study was supported by grants awarded to SN.
Manuscript received on December 23, 2011. Revised version arrived on May 6, 2012. Manuscript accepted on June 7, 2012.
Correspondence: Shinji Nakao, MD, PhD, Cellular Transplantation Biology, Kanazawa University Graduate School of Medical Science, 13-1 Takaramachi, Kanazawa, Ishikawa 920-8640, Japan. Phone: international +81.76.2652274. Fax: international +81.76.2344252.
E-mail: snakao8205@staff.kanazawa-u.ac.jp

refractory cytopenia with multilineage dysplasia (RCMD) and 60 with MDS-U, whose blood samples were sent to our laboratory between May 1999 and July 2010 for screening of GPI-AP$^-$ granulocytes and erythrocytes. BM smear slides were reviewed by 2 independent hematologists. BM cellularity was defined as the percentage of BM volume occupied by hematopoietic cells in the trephine biopsy specimens. Hypocellular marrow was defined as less than 30% cellularity in patients under the age of 70 years, or less than 20% cellularity in patients 70 years and over.[6] Chromosomal analysis was performed and described according to the International System for Human Cytogenetic Nomenclature (ISCN).[7] Responses to IST were defined according to the established criteria.[8] The ethics committee of Kanazawa University Graduate School of Medical Science approved the study protocol, and all patients provided their informed consent prior to sampling.

Monoclonal antibodies

Monoclonal antibodies (mAbs) used for flow cytometry are shown on the *Online Supplementary Table S1*.

Flow cytometry for detecting GPI-AP$^-$ cells

All blood samples were analyzed within 24 h of collection to avoid false positive results due to cell damage. Staining with each mAb was performed according to the lyse-stain protocol as previously described.[5,9] The presence of CD55$^-$CD59$^-$glycophorin A$^+$ erythrocytes at the level of 0.005% and over and/or CD55$^-$CD59$^-$CD11b$^+$ granulocytes at the level of 0.003% or over was defined as an abnormal increase ('positive') based on the results obtained from 183 healthy individuals.[10] With careful handling of samples and elaborate gating strategies, cut-off values can be lowered to these levels without producing false positive results.[10-12]

Cell sorting and FISH analysis

GPI-AP$^+$ and GPI-AP$^-$ granulocytes from 2 patients with del(13q) (unique patient numbers (UPNs) 3 and 7) were sorted using a FACSAria III cell sorter (BD Bioscience, Franklin Lakes, NJ, USA) and subjected to fluorescence *in situ* hybridization (FISH) analysis using a D13S319-specific probe (Vysis, Voisins-le-Bretonneux, France) as previously described.[13]

Genome analysis of deleted region in patients with del(13q)

Genomic DNA was isolated from peripheral blood cells of 7 patients with del(13q) (UPNs 1, 3, 4, 5, 7, 8 and 22) and subjected to SNP array-based genome-wide analysis of genetic alterations using GeneChip® 250K arrays (Affymetrix, Santa Clara, California, USA) according to the manufacturer's protocol. Genomic and allele-specific copy numbers were calculated using Copy Analyser for GeneChip® (CNAG) software as previously described.[14,15]

Statistical analysis

Prevalence of increased GPI-AP$^-$ cells among different patient populations was compared using the χ^2 test. Time-to-event variables were analyzed using the Kaplan-Meier method, and groups were compared with the log rank test. Two-sided *P* values were calculated and $P<0.05$ was considered statistically significant. All statistical analyses were performed using the JMP software program version 8.0 (SAS Institute, Cary, NC, USA).

Results and Discussion

Of the 1,228 patients with BM failure, 22 possessed del(13q) (1.8%) that were demonstrated by G-banding; their clinical features are summarized in Table 1. Sixteen patients had only the del(13q) abnormality (which we define as 13q-^{alone}) while the remaining 6 patients had other abnormalities, which we define as 13q^{+other}. Of these 6, 2 had -Y, one had -20, one had del(7q), one had +8, and one had +mar in addition to the del(13q) abnormality. The presence of the del(13q) clone was confirmed by FISH when the number of del(13q) revealed by the G-banding method was less than or equal to two. Median age was 64.5 years old, and BM was hypocellular in 16 patients (12 with 13q^{-alone} and 4 with 13q^{+other}), normocellular in 4 (2 with 13q^{-alone} and 2 with 13q^{+other}), not evaluable in 2 with 13q^{-alone}. All patients with del(13q) were diagnosed with MDS-U due to the absence of significant dysplasia that would fulfill the criteria for MDS as defined by the 2008 WHO classification. All patients were classified as Int-1 according to the International Prognostic Scoring System (IPSS), except for UPN17 who had an IPSS score of 1.5 (Int-2).

As shown in Table 1, GPI-AP$^-$ cells that accounted for from 0.006% to 12.342% (median 0.137%) of granulocytes were detected in all 16 13q^{-alone} patients. FISH analysis of sorted GPI-AP$^-$ and GPI-AP$^+$ granulocytes revealed that del(13q) cells were derived from non-*PIGA* mutant hematopoietic stem cells (HSCs) (Figure 1A). On the other hand, the prevalence of elevated GPI-AP$^-$ cell percentages in 13q^{+other} patients and those with a normal karyotype (637 patients with AA and 300 with MDS) was 50% (3 of 6) and 43% (405 of 937), respectively ($P<0.001$).

Fourteen 13q^{-alone} patients were treated with cyclosporine (CsA) alone,[6] CsA and antithymocyte globulin (ATG)[6] or CsA and anabolic steroids;[2] all achieved either a hematologic improvement in two or three lineages or complete remission (CR), while the response rate to IST in 13q^{+other} patients was 40%. No case was IST-dependent, and response was durable after the cessation of the treatment after patients achieved CR. The clinical course of one patient (UPN 4) who responded to CsA alone and entered CR, despite the fact that G-banding of BM cells showed all 20 dividing cells to be del(13q), has been previously reported.[16] Ninety-six AA patients with the normal karyotype were treated with CsA and ATG (n=47) or CsA±anabolic steroids (n=49). Seventy-eight percent of AA patients responded to IST. Among 19 MDS patients (RCUD, n=14; RCMD, n=5) with a normal karyotype who have been treated with ATG plus CsA (n=3) or CsA with or without anabolic steroids (n=16), 63% responded to IST.

None of the 17 13q^{-alone} patients progressed to advanced MDS or acute myeloid leukemia (AML) during the follow-up period of 3-108 months (median 52 months), while 2 of 6 13q^{+other} patients (one with -20, one with del(7q)) developed AML. The 10-year overall survival rates of patients with 13q^{-alone}, patients with 13q^{+other}, AA patients with a normal karyotype and MDS (RCUD, n=38; RCMD, n=20; MDS-U, n=8) patients with a normal karyotype were 83%, 67%, 85% and 57%, respectively ($P=0.0003$, log rank test on 3 degrees of freedom) (Figure 1B). The 10-year overall survival rates of AA patients with a normal karyotype with and without increased GPI-AP$^-$ cells and MDS (38 with RCUD, 20 with RCMD and 8 with MDS-U) patients with a normal karyotype with and without increased GPI-AP$^-$ cells were 85%, 84%, 66% and 55%, respectively ($P=0.0011$, log rank test on 4 degrees of freedom) (Figure 1C). The percentage of del(13q) clones revealed by G-banding increased in 5 patients and decreased in 3 after successful IST. (*Online Supplementary*

Figure S1) No patient developed clinical features of paroxysmal nocturnal hemoglobinuria (PNH).

SNP array analysis of peripheral blood cells from 7 $13q^{-alone}$ and $13q^{-other}$ patients indicated the region from 13q13.3 to 13q14.3 to be commonly deleted (Figure 1D).

The current retrospective study with a large number of BM failure patients revealed distinctive clinical features of BM failure with del(13q) abnormalities. The 1.8% incidence of del(13q) patients was comparable to that of a recent study (1.9%) based on 2,072 patients with MDS,[17] for which detailed diagnoses of patients with del(13q) were not provided. All del(13q) patients in our study were classified as MDS-U due to the absence of significant dysplasia. We have previously reported that response to IST was remarkably high in 9 patients with del(13q). The present study, which used a different patient cohort, confirmed our previous finding.[2] Between these 22 patients and the 9 patients that we reported in 2002, only 2 developed AML and 22 responded to IST. The overall and leukemia-free survival spans of del(13q) patients treated with IST were as long as AA patients with normal karyotypes treated with IST. These findings suggest that the del(13q) clone in BM failure patients represents the presence of immune pathophysiology rather than clonal disorder associated with AML risk.

Table 1. Clinical features of bone marrow failure patients with del(13q) alone (patients 1-16) or del(13q) plus other abnormalities (patients 17-22).

UPN	Age (years)	Sex	Months from diagnosis to sampling	Dysplasia	Cellularity	Cytogenetics	% of del(13q) cells	Break point	% GPI(-) granulocytes	% GPI(-) RBCs	Previous therapy	Treatment	Response	Outcome	AML transformation	LFS (months)
1	64	F	54	None	hypo	46,XX,del 4/20 (13)(q?)	20	13q(?)	0.042	0.015	No	CsA+AS	HI-2	alive	No	67+
2	42	M	0	None	hypo	46,XY,del(13)(q12q14) 1/20	5	13(q12q14)	3.511	0.562	No	CsA	CR	alive	No	79+
3	47	F	0	None	hypo	46,XX, del(13)(q?) 2/20	10	13q(?)	2.101	0.601	No	ATG+CsA	HI-3	alive	No	24+
4	50	F	4	Erythroid	hypo	46,XX,del(13)(q12q22) 20/20	100	13(q12q22)	0.111	0.013	No	CsA	CR	alive	No	44+
5	65	F	5	None	hypo	46,XX,del(13)(q12q14) 3/20	15	13(q12q14)	0.009	0.008	No	ATG+CsA	CR	alive	No	43+
6	21	M	1	None	hypo	46,XY, del(13)(q?) 6/20	30	13q(?)	0.038	0.003	No	ATG+CsA	HI-3	alive	No	15+
7	52	M	1	Erythroid	NE	46,XY, del(13)(q?) 19/20	95	13q(?)	12.342	0.524	PSL	CsA	HI-3	alive	No	3+
8	87	F	1	None	normo	46,XX,del(13)(q12q22) 9/20	45	13(q12q22)	0.37	0.095	No	CsA	HI-3	alive	No	15+
9	63	F	16	None	hypo	46,XX,del(13)(q12q14) del(13)(q21q31) 5/20	25	13(q12q14), 13(q21q31)	0.006	0.665	PSL	ATG+CsA	HI-3	alive	No	29+
10	74	F	3	None	hypo	46,XX, del(13)(q12q14) 7/13	54	13(q12q14)	0.504	N/A	No	ATG+CsA	HI-3	death (cancer)	No	38
11	54	F	0	None	hypo	46,XX,del(13)(q14q22) 40/40	100	13(q14q22)	0.125	0.008	No	Allo-BMT	NE	alive	No	74+
12	53	M	43	None	hypo	46,XY,del(13)(q14.3)	14	13q14.3	0.281	0.539	No	ATG+CsA	HI-3	alive	No	108+
13	85	M	1	None	hypo	46,XY,del(13)(q?) 2/20	10	13q(?)	0.031	0.01	No	No treatment	NE	death	No	10
14	77	F	3	Erythroid	NE	46,XX,del(13)(q?) 8/20	40	13q(?)	3.125	1.65	No	CsA	CR	alive	No	45+
15	56	M	1	Erythroid	normo	46,XX,del(13)(q12q14) 6/20	30	13(q12q14)	0.069	0.036	No	CsA	HI-2	alive	No	24+
16	74	M	37	None	hypo	46,XY,del(13)(q?) 7/20, 47,X,+Y 7/20	35	13q(?)	0.171	0.441	No	CsA+AS	HI-2	alive	No	52+
17	69	M	1	None	hypo	46,XY,del(7)(q22), del(13)(q12q14) 3/20	15	13(q12q14)	0	0	No	CsA+AS	NR	death	Yes	8
18	68	F	1	None	normo	45,XX,del(13)(q12q22),-20 2/20	10	13(q12q22)	0	0	No	VitK	NE	death	Yes	7
19	75	M	2	None	hypo	45,X,-Y,del(13)(q?) 2/20	10	13q(?)	0	0.003	PSL	CsA	NR	alive	No	71+
20	81	M	17	None	hypo	47,XY,+8,del(13)(q?) 19/20	95	13q(?)	6.851	0.272	No	CsA	NE	alive	No	67+
21	57	F	122	Erythroid	normo	46,XX,del(13),+mar 10/20	50	del(13)	0.522	1.075	AS	CsA+AS	HI-3	alive	No	146+
22	66	M	1	Erythroid	hypo	45,X,-Y,del(13)(q12q14) 15/20	75	13(q12q14)	0.149	0.209	No	CsA	HI-2	alive	No	11+
Median	**65**						**30**		**0.137**	**0.095**						

UPN: unique patient number; M: male; F: female; normo: normocellular marrow; hypo: hypocellular marrow; GPI-AP-granulocytes, glycosylphosphatidyl-inositol anchored protein-deficient granulocytes; GPI-AP-erythrocytes, glycosylphosphatidyl-inositol anchored protein-deficient erythrocytes; CsA: cyclosporine; ATG: antithymocyte globulin; AS: anabolicsteroid; Allo-BMT: allogeneic bone marrow transplant; VitK: vitamin K; CR: complete remission; HI-2: hematologic improvement in two lineages; HI-3: hematologic improvement in three lineages; NR: no response; NE: not evaluable; AML: acute myeloid leukemia; LFS: leukemia-free survival.

Transformation of patient 17 (UPN17) to AML could be attributed to the coexistence of del(7q), which is associated with high risk of AML evolution.[18]

The percentage change of del(13q) clone following IST varied from one patient to another (*Online Supplementary Figure S1*) in a similar way in which the percentage of GPI-AP$^-$ cells changed in the present study (*data not shown*), which is consistent with our previous findings regarding *PIGA* mutant HSCs.[10] Given that effective removal of immune mechanisms by IST does not consistently lower the percentage of del(13q) clone, it is speculated that preferential expansion of del(13q) clones by the immune mechanisms at the onset of BM failure[10] may lead to the escape from immunological pressure, as in the case of *PIGA*

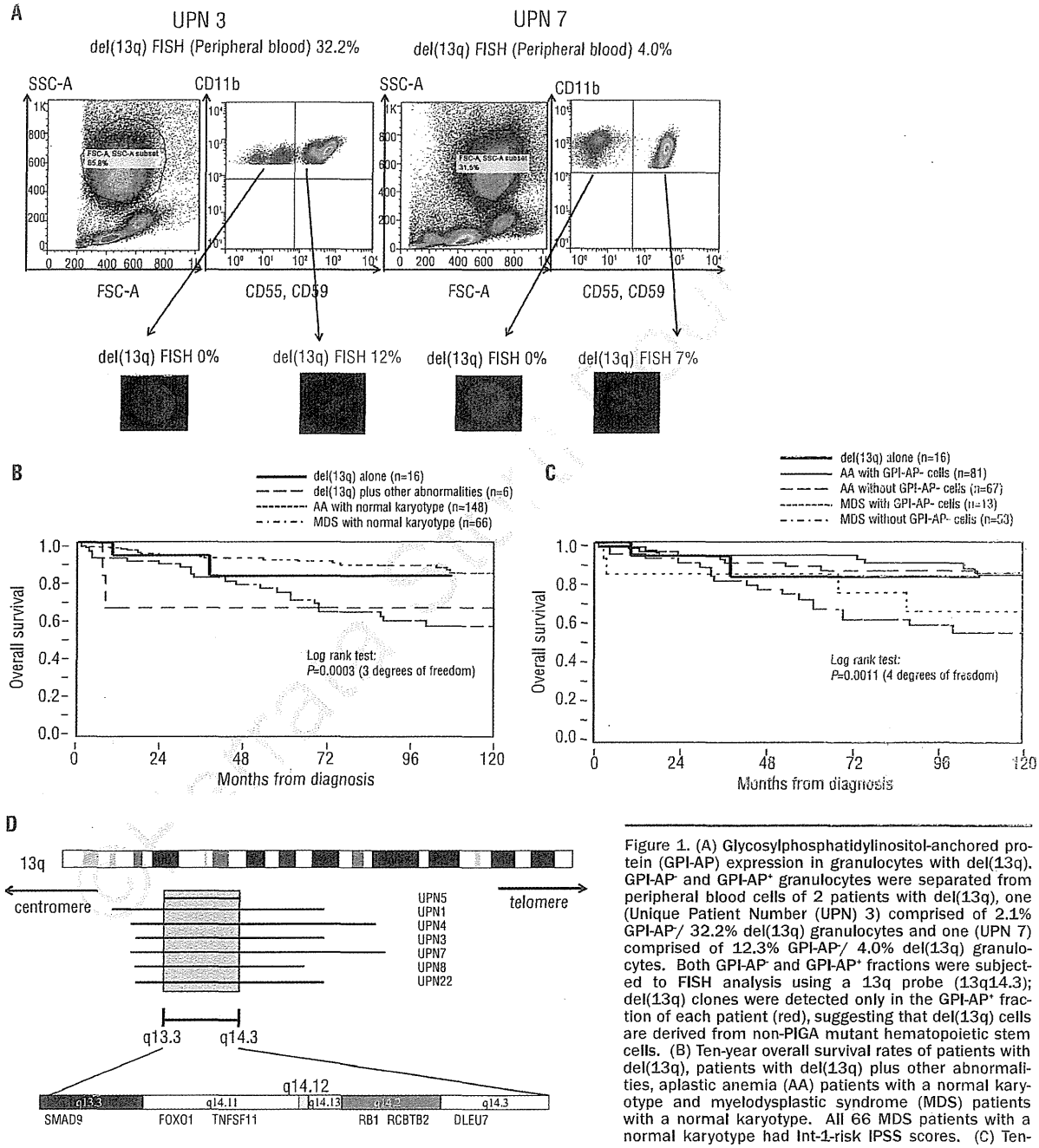

Figure 1. (A) Glycosylphosphatidylinositol-anchored protein (GPI-AP) expression in granulocytes with del(13q). GPI-AP$^-$ and GPI-AP$^+$ granulocytes were separated from peripheral blood cells of 2 patients with del(13q), one (Unique Patient Number (UPN) 3) comprised of 2.1% GPI-AP$^-$/ 32.2% del(13q) granulocytes and one (UPN 7) comprised of 12.3% GPI-AP$^-$/ 4.0% del(13q) granulocytes. Both GPI-AP$^-$ and GPI-AP$^+$ fractions were subjected to FISH analysis using a 13q probe (13q14.3); del(13q) clones were detected only in the GPI-AP$^+$ fraction of each patient (red), suggesting that del(13q) cells are derived from non-PIGA mutant hematopoietic stem cells. (B) Ten-year overall survival rates of patients with del(13q), patients with del(13q) plus other abnormalities, aplastic anemia (AA) patients with a normal karyotype and myelodysplastic syndrome (MDS) patients with a normal karyotype. All 66 MDS patients with a normal karyotype had Int-1-risk IPSS scores. (C) Ten-year overall survival rates of patients with del(13q), aplastic anemia (AA) patients with a normal karyotype with and without increased GPI-AP$^-$ cells and myelodysplastic syndrome (MDS) patients with a normal karyotype with and without increased GPI-AP$^-$ cells. (D) Deleted gene loci regions of 7 patients with del(13q), shown as bold horizontal lines for each UPN under the gene. The shaded box represents the deleted region common to patients, 13q13.3 to 13q14.3, which encodes proteins involved in cytokine signal transduction.

mutant HSCs. It is necessary to identify common mechanisms leading to preferential activation of both PIGA mutant HSCs and HSCs with del(13q) in immune-mediated BM failure to verify these hypotheses.

A possible immune pathophysiology in $13q^{-alone}$ patients is supported by the markedly high prevalence (100%) of elevated GPI-AP$^-$ cell levels which is linked to the escape of *PIGA* mutant HSCs from an immune system attack.[19] Because the del(13q) abnormality occurs in the GPI-AP$^+$ population, it may play a similar role to the GPI-AP$^-$ cells. SNP array analysis revealed the common deletion of a 15 Mb (13.3 to 14.3) region of 13q in 7 $13q^{-alone}$ and $13q^{-other}$ patients. This segment encodes several proteins that regulate cell proliferation and the cell cycle, such as SMAD9 and RB1; both are involved in the signal transduction pathway of transforming growth factor-beta (TGF-β, an important cytokine in regulating HSC dormancy. Cytokine-mediated selection of *PIGA* mutant HSCs has been proposed as a mechanism for preferential proliferation of GPI-AP$^-$ cells,[20] but no supporting evidence has been presented. A previous study demonstrated that GPI-AP$^-$ T cells show decreased sensitivity to herpes virus entry mediator (HVEM) ligands that transmit inhibitory signals through receptors for CD160(21) and TGF-β.[22,23] The presence of del(13q) represents a unique subgroup of immune-mediated BM failure associated with an increase in the percentage of GPI-AP$^-$ cells, where del(13q) and *PIGA* mutant HSCs undergo preferential expansion, possibly due to their decreased sensitivity to cell-cycle inhibitory molecules, such as TGF-β compared to normal HSCs.

In conclusion, MDS-U with del(13q) alone is a benign BM failure syndrome characterized by a good response to IST and a markedly high prevalence of elevated GPI-AP$^-$ cell percentages. Therefore, del(13q) should be eliminated from the list of karyotypic abnormalities representing the intermediate group defined by IPSS,[24] and BM failure with del(13q) should be managed as AA.

Authorship and Disclosures

The information provided by the authors about contributions from persons listed as authors and in acknowledgments is available with the full text of this paper at www.haematologica.org.

Financial and other disclosures provided by the authors using the ICMJE (www.icmje.org) Uniform Format for Disclosure of Competing Interests are also available at www.haematologica.org.

References

1. Schanz J, Steidl C, Fonatsch C, Pfeilstocker M, Nosslinger T, Tuechler H, et al. Coalesced multicentric analysis of 2,351 patients with myelodysplastic syndromes indicates an underestimation of poor-risk cytogenetics of myelodysplastic syndromes in the international prognostic scoring system. J Clin Oncol. 2011;29(15):1963-70.
2. Ishiyama K, Karasawa M, Miyawaki S, Ueda Y, Noda M, Wakita A, et al. Aplastic anaemia with 13q-: a benign subset of bone marrow failure responsive to immunosuppressive therapy. Br J Haematol. 2002;117 (3):747-50.
3. Sloand EM, Olnes MJ, Shenoy A, Weinstein B, Boss C, Loeliger K, et al. Alemtuzumab treatment of intermediate-1 myelodysplasia patients is associated with sustained improvement in blood counts and cytogenetic remissions. J Clin Oncol. 2010;28(35): 5166-73.
4. Wang H, Chuhjo T, Yasue S, Omine M, Nakao S. Clinical significance of a minor population of paroxysmal nocturnal hemoglobinuria-type cells in bone marrow failure syndrome. Blood. 2002;100(12):3897-902.
5. Sugimori C, Chuhjo T, Feng X, Yamazaki H, Takami A, Teramura M, et al. Minor population of CD55-CD59- blood cells predicts response to immunosuppressive therapy and prognosis in patients with aplastic anemia. Blood. 2006;107(4):1308-14.
6. Yue G, Hao S, Fadare O, Baker S, Pozdnyakova O, Galili N, et al. Hypocellularity in myelodysplastic syndrome is an independent factor which predicts a favorable outcome. Leuk Res. 2008; 32(4):553-8.
7. International Standing Committee on Human Cytogenetic Nomenclature. Shaffer LG, Slovak ML, Campbell LJ. ISCN 2009: an international system for human cytogenetic nomenclature (2009). Basel; Unionville, CT: Karger; 2009. vi, 138.
8. Cheson BD, Greenberg PL, Bennett JM, Lowenberg B, Wijermans PW, Nimer SD, et al. Clinical application and proposal for modification of the International Working Group (IWG) response criteria in myelodysplasia. Blood. 2006;108(2):419-25.
9. Araten DJ, Nafa K, Pakdeesuwan K, Luzzatto L. Clonal populations of hematopoietic cells with paroxysmal nocturnal hemoglobinuria genotype and phenotype are present in normal individuals. Proc Natl Acad Sci USA. 1999;96(9):5209-14.
10. Sugimori C, Mochizuki K, Qi Z, Sugimori N, Ishiyama K, Kondo Y, et al. Origin and fate of blood cells deficient in glycosylphosphatidylinositol-anchored protein among patients with bone marrow failure. Br J Haematol. 2009;147(1):102-12.
11. Kulagin A, Golubovskaya I, Ganapiev A, Babenko E, Sipol A, Pronkina N, et al. Prognostic value of minor PNH clones in aplastic anaemia patients treated with ATG-based immunosuppression: results of a two-centre prospective study. Bone Marrow Transplant. 2011;46:S83-S4.
12. Parker C, Omine M, Richards S, Nishimura J, Bessler M, Ware R, et al. Diagnosis and management of paroxysmal nocturnal hemoglobinuria. Blood. 2005;106(12):3699-709.
13. Facon T, Avet-Loiseau H, Guillerm G, Moreau P, Genevieve F, Zandecki M, et al. Chromosome 13 abnormalities identified by FISH analysis and serum beta2-microglobulin produce a powerful myeloma staging system for patients receiving high-dose therapy. Blood. 2001;97(6):1566-71.
14. Nannya Y, Sanada M, Nakazaki K, Hosoya N, Wang L, Hangaishi A, et al. A robust algorithm for copy number detection using high-density oligonucleotide single nucleotide polymorphism genotyping arrays. Cancer Res. 2005;65(14):6071-9.
15. Yamamoto G, Nannya Y, Kato M, Sanada M, Levine RL, Kawamata N, et al. Highly sensitive method for genomewide detection of allelic composition in nonpaired, primary tumor specimens by use of affymetrix single-nucleotide-polymorphism genotyping microarrays. Am J Hum Genet. 2007;81(1): 114-26.
16. Kasahara I, Nishio M, Endo T, Fujimoto K, Koike T, Sugimori N, et al. Sustained trilineage hematopoietic recovery in a patient with refractory anemia, del(13)(q12q22), and paroxysmal nocturnal hemoglobinuria-type cells treated with immunosuppressive therapy. Leuk Res. 2011;35(9):e147-8.
17. Haase D. Cytogenetic features in myelodysplastic syndromes. Ann Hematol. 2008;87 (7):515-26.
18. Maciejewski JP, Risitano A, Sloand EM, Nunez O, Young NS. Distinct clinical outcomes for cytogenetic abnormalities evolving from aplastic anemia. Blood. 2002;99(9): 3129-35.
19. Rotoli B, Luzzatto L. Paroxysmal nocturnal haemoglobinuria. Baillieres Clin Haematol. 1989;2(1):113-38.
20. Parker CJ. The pathophysiology of paroxysmal nocturnal hemoglobinuria. Exp Hematol. 2007;35(4):523-33.
21. Cai G, Anumanthan A, Brown JA, Greenfield EA, Zhu B, Freeman GJ. CD160 inhibits activation of human CD4+ T cells through interaction with herpesvirus entry mediator. Nat Immunol. 2008;9(2):176-85.
22. Yamazaki S, Iwama A, Takayanagi S, Eto K, Ema H, Nakauchi H. TGF-beta as a candidate bone marrow niche signal to induce hematopoietic stem cell hibernation. Blood. 2009;113(6):1250-6.
23. Katagiri T, Qi Z, Ohtake S, Nakao S. GPI-anchored protein-deficient T cells in patients with aplastic anemia and low-risk myelodysplastic syndrome: implications for the immunopathophysiology of bone marrow failure. Eur J Haematol. 2011;86(3):226-36.
24. Greenberg P, Cox C, LeBeau MM, Fenaux P, Morel P, Sanz G, et al. International scoring system for evaluating prognosis in myelodysplastic syndromes. Blood. 1997;89 (6):2079-88.